Emerging OCDMA communication systems and data networks [Invited]

Jawad A. Salehi

Optical Networks Research Laboratory, Advanced Communication Research Institute, Electrical Engineering Department, Sharif University of Technology, Tehran 11365-9363, Iran
jasalehi@sharif.edu

Received April 10, 2007; revised July 8, 2007; accepted July 13, 2007; published August 28, 2007 (Doc. ID 81958)

I present an in-depth review of the trends and the directions taken by researchers worldwide in optical code-division multiple-access (OCDMA) systems. I highlight those trends and features that I believe are essential to the successful introduction of various OCDMA techniques in communication systems and data networks in the near future. In particular I begin by giving a comprehensive review of the construction of optical orthogonal codes (OOCs). Specifically I discuss the recently developed algorithms that are based on matrix algebra, which simplify and enhance the efficiencies of algorithms in OOC generation. In communication systems studies I first focus on and discuss various OCDMA techniques, such as incoherent and coherent OCDMA. A comprehensive discussion takes place on all important aspects of each OCDMA technique. In particular, I elaborate on enabling technologies that are needed prior to full scale consideration of OCDMA in communication systems. For incoherent OCDMA the technique is categorized into two distinguished techniques, namely, 1D and 2D OCDMA. For each technique I discuss the various receiver structures proposed to date. In particular I discuss a recently introduced powerful receiver structure based on optical AND logic gate elements. Based on this receiver structure I conclude that in many practical applications, OOCs with a cross-correlation value λ equal to 2 or 3, which have a much larger cardinality compared to OOCs with $\lambda=1$, perform much better. Many fundamental issues, including architectural consideration of multiple amplifiers, various acquisition algorithms, and advanced signaling methods, such as pulse position modulation, are discussed. For coherent OCDMA or spectrally encoded ultrashort light pulse OCDMA, I begin by having an in-depth discussion on the key and enabling technologies that are essential in the successful implementation of this very important and extremely powerful technique. In particular on the encoder–decoder side I present discussions on various key device technologies such as virtually imaged pulsed array, fiber Bragg gratings, and arrayed waveguide gratings. On the receiver side I elaborate on various nonlinear detection schemes used in such OCDMA networks. I will present an analytical framework on the above nonlinear detection schemes and discuss their pros and cons. I extend the discussion to various data networks. In particular I will discuss applications such as wireless OCDMA LAN, free-space OCDMA, fiber-to-the-home, and other code-division-multiple-access-based packet communication networks using label addressing and processing techniques to indicate the directions and the applications for which OCDMA systems are considered. It is believed that in the not so distant future OCDMA, once fully developed and matured, will be an inseparable part of advanced optical communication systems and networks, due to its various desirable features and functionalities.

OCIS codes: 060.2330, 060.4510, 060.1660.

1. Introduction

It was almost 18 years ago when I was asked to write what was probably the first review paper on an obscure and little known multiple-access technique; namely, optical code-division multiple access (OCDMA) [1]. I am quite pleased today that after 18 years I find myself having another opportunity to write a review paper on this very well-known and established optical multiple-access technique. This time I am not discussing only the techniques themselves but rather the communication systems and the data networks that are envisioned to arise from these very advanced and exciting techniques. So it is fair to conclude that, because of their immense potential and

clever encoding and decoding mechanisms that are essential for future all-optical communication systems and data networks, OCDMA techniques have finally succeeded in capturing the imaginations, the beliefs, and the trust of many communication and optical scientists, engineers, and technologists.

The lag in recognizing the potential of OCDMA techniques came not from the conceptual development, but rather from the enabling and advancing photonics to support the fundamental functionalities needed in developing OCDMA-based communication and data systems. For me it was always the case that the conceptual developments of OCDMA techniques were far ahead of the corresponding technologies needed in optics and photonics for their support. It was not surprising, then, that this was indeed the case since the introduction of powerful all-optical code-division multiple-access (CDMA) techniques caught everyone within the community by surprise. The elegant solutions that were introduced were so exciting and so fundamental to light properties and optical channels that even the opponents of OCDMA were respectful of it. Today, however, things are different. Many advance photonic devices are getting developed rapidly and significant strides on all-optical signal processing and nonlinear optics which are at the heart of any communication and data system, have been made. In fact today it seems that the table is turned against rapid conceptual advancement and there is this fear that device advancement has a faster pace than that of the conceptual development required for their proper and efficient use in OCDMA-based systems.

The legacy of OCDMA seems to follow that of wireless- and mobile-based CDMA communication systems, which were introduced almost 16 years ago for the first time. The success of CDMA-based wireless transmission and communication systems is owed first to the maturing device integration and second to the high-level network concepts, features, and requirements. In cellular networks the features of soft-blocking and soft-hand off, with no dynamic frequency allocation offered by the CDMA technique, were essential to increase the capacity and the number of users of bursty networks with no degradation in overall system performance.

Today reading through thousands of research papers, theoretical and experimental, on OCDMA it becomes clear that OCDMA techniques are sought after due to their abilities to support many asynchronous bursty transmissions without any delay and network control, not to mention the high-level of security it may offer to casual users. Given that optical bandwidth is abundant the needed processing gain is within the realm of any optical communication system. How to use this abundant bandwidth to reduce network complexity and hence the access cost is what OCDMA is all about [2].

In this paper we will review the developments taken for the past 18 years in OCDMA worldwide. It is almost impossible to cover all developments in the past 18 years due to the rapid expansion and proliferation of literature on OCDMA techniques and systems. Hence I will focus on and highlight those trends and features that I believe are essential to the successful introduction of the OCDMA technique in communication systems and data networks.

This paper is organized as follows. Section 2 discusses advance algorithms in generating optical orthogonal codes (OOCs). I especially highlight the importance of OOCs with cross-correlation values greater than one for future incoherent OCDMA systems. Section 3 describes various OCDMA systems using OOCs. In particular I discuss advanced receiver structures introduced to date, such as receivers using optical AND logic gate structures. I further elaborate on 2-D OCDMA systems proposed recently by many research groups. Section 4 discusses an advance OCDMA system using spectral phase encoding and decoding techniques and discusses enabling technologies that are needed to support such systems. In particular I describe various nonlinear threshold elements proposed for such systems and discuss the pros and cons of each. Section 5 focuses mainly on various OCDMA-based data networks and communication systems. Various code translation, code add–drop, and OCDMA driven networking are discussed. Furthermore, we discuss interesting wireless OCDMA-based LANs and free-space atmospheric communication systems.

A personal note. For me it all began when I was invited to be interviewed at Bell Communications Research (Bellcore) on a beautiful spring day in 1984 by a visionary man, none other than Charles (Chuck) A. Brackett, the former head of the optical multiple-access network group at Bellcore in Piscataway, New Jersey. Typical to the old Bell Laboratories's tradition, a Ph.D candidate begins the interview day by pre-

senting his or her doctoral thesis. My doctoral thesis was supervised by Charles L. Weber and Robert A. Scholtz, both pioneers in spread-spectrum techniques, at the University of Southern California (USC). It focused on evaluating the performance of what was then a promising multiple-access technique, namely, CDMA in wireless and mobile communication channels. Throughout my thesis, I learned all about various CDMA techniques such as direct-sequence spreading and frequency and time hopping. I also learned how to apply and model the various techniques in typical mobile and wireless communication systems. At that time USC was among the best centers of research in spread-spectrum communication techniques. Indeed, if one looks back at the early 1980s at the Communication Sciences Institute (CSI), great names such as Solomon Golomb, Irving Reed, Robert Scholtz, Charles Weber, William Lindsey, Robert Gagliardi, and Lloyd Welch appeared among its faculty members, so it is no wonder USC was considered the mecca of spread-spectrum techniques in the world, which by the early 1990s had a direct impact on the multi-billion-dollar industry in wireless and mobile communications worldwide.

I was extremely fortunate and lucky to have been a graduate student at such a place at the time when the CDMA technique, an obscure notion to most other research laboratories and universities, including Bell Laboratories, was at the forefront of research activities for mobile and wireless communication systems at CSI–USC. The culture at Bell Laboratories and most other telephone companies with respect to multiple-access techniques was based simply on time- or frequency-division multiple access. The concepts and the notions of the CDMA technique in most telecommunication companies were almost nonexistent. At the end of my doctoral thesis presentation, I was asked by Brackett whether I could think of applying the CDMA technique to optical channels. His argument was that we have an extraordinary amount of bandwidth in optical-fiber channels that can be used as the needed degrees of freedom (processing gain) to establish CDMA techniques. However, as he further argued, what will distinguish OCDMA from classical radio communications would be in performing the necessary signal processing requirements such as encoding, decoding, multiplexing, demultiplexing, etc. all in optical domain. He concluded his argument by stating that it is well known that optical devices and all-optical processing can handle and process a lot more bandwidth than their electronic counterparts.

There were, of course, some key papers that were needed to be understood first in order to tackle CDMA techniques in optical domain. The first and foremost was a paper written by a group of researchers at Stanford University led by Moslehi *et al.* [3]. The second was a short note written by Davies and Shaar [4], and the third was a paper by Marom [5], which later was crucial in helping me to formulate a new class of codes, namely OOCs. The paper by Moslehi *et al.* [3] was an in-depth study of fiber-optics lattice signal processing theory and implementation. It was in that paper that the theory of unipolar systems, a fundamental theory that puts the limits on how much should we expect from such systems, was addressed. An example of such systems is intensity-modulation–direct-detection optical communication systems. In a simple language the theory of unipolar systems states that one can only use signals based on positive real numbers in the design and processing of such systems. The paper by Davies and Shaar [4] highlighted for the first time, to the best of my knowledge, the nature and the role of optical channel (an OR channel) in the OCDMA environment. It is fair to say that this paper gave the first insight on how one had to approach and look at the problem from the right perspective.

However for me the paper by Marom [5], in which he attempts to implement an optical tapped-delay line to recognize sequences with good autocorrelation in optical domain for certain communication applications such as synchronization and signal detection, played a major role. To obtain satisfactory results Marom [5] introduced an optical sequence with a structure that took into account time domain chirped effect. Chirping in time requires that subsequent pulses be separated in time domain by an integer multiple of the minimum time separation and no time separation can be repeated. By doing so he succeeded in showing a decoded optical sequence with a peak value equal to the number of pulses in the sequence and sidelobe values that were bounded by one, the minimum possible sidelobe value in any given positive system. The notion that no two pulses in the sequence may have equal time separation played a central role and helped me to design and introduce for the first time, to the best of my knowledge, a whole new class of multiple-access codes, namely, OOCs [6,7]. The

fundamental structures and rules in introducing these codes were presented to a group of researchers at Bellcore in March 1985. This prompted the collaboration between Chung, Wei, and myself to devise various generating algorithms for these newly introduced OOCs [8]. Today OOCs are well established and are a highly researched topic by various mathematical societies and sequence designers. By spring 1985 we had a running experiment demonstrating the principles of the OCDMA technique using OOCs.

To the best of my knowledge Hui (Bellcore) [9], Prucnal *et al.* (Columbia University) [10], and Foschini and Vannucci (Bell Laboratories) [11] were the other researchers in the world, beside myself, who were pursuing the same line of research at the same time. Hui proposed multifiber OCDMA [9]. Prucnal's work, however, did succeed in showing the roles of fiber-optic tapped-delay lines in encoding and decoding prime sequences for OCDMA systems [10]. However, it was the introduction of OOCs with their elegant and challenging characteristics and mathematical structures that are fundamental and natural to incoherent light pulses that generated much interest among researchers worldwide to explore the possibilities of OCDMA techniques for future all-optical multiple-access communication systems.

When the results of OOC-based OCDMA were exposed to our colleagues at Bellcore, a group of researchers at Navesink, New Jersey, namely, J. P. Heritage, A. M. Weiner, and R. N. Thurston under the supervision of Peter Smith—another visionary scientist—approached me and Brackett to discuss the possible use of their optical apparatus for communications and multiple-access purposes. The optical apparatus developed by the group was primarily used for various optical pulse shaping applications using as its input coherent ultrashort light pulses generated by a mode-locked laser. These ultrashort light pulses had radically different characteristics when compared to incoherent optical pulses. With coherent mode-locked pulses we had the ability to manipulate the phase of the harmonics of the optical pulses in order to generate more complex and extremely featured pulses in time domain. After studying the apparatus known as 4F, we were able to show for the first time the encoding and decoding of femtosecond pulses in the context of an OCDMA system [12,13]. This was considered a major breakthrough in the field of OCDMA worldwide. For me, the key to succeeding in introducing this clever technique, namely, femtosecond or coherent ultrashort light pulse CDMA, was the realization that the 4F apparatus holds three fundamental mathematical functions: Fourier transformation, spectral multiplication, and inverse Fourier transformation. With this building block then the notion of femtosecond CDMA was relieved from 4F apparatus and indicated that any device that can carry the above three fundamental mathematical functions can be employed for such a technique. Another surprising element of this technique was the mathematical model that followed and with which the system performance was analyzed. The mathematical model that was introduced bypassed light and device physics altogether in order to highlight the essential parameters that do matter in system analysis, such as the number of users, code length, threshold, processing gain, and bit rate. The analysis on these systems shows that an OCDMA system designed based on this technique can have throughputs as high as hundreds of gigabits per second.

Spectrally encoded OCDMA removed the limitations and the bottlenecks that existed with positive OCDMA systems, and it is the optical counterpart of direct-sequence CDMA systems used in radio and mobile communication systems. Today, for the most part, it can use pseudorandom sequences generated by maximal-length shift registers: the same class of sequences used for mobile and wireless communications. I have no doubt that as the enabling optical devices mature the spectrally encoded femtosecond CDMA technique will become the dominant technique in fiber-optic-based communication systems due to its powerful ability to establish the fastest and highest flow of data in any OCDMA system. Today with the advent of various optical devices such as array-waveguide gratings (AWG), fiber Bragg grating (FBG), virtually imaged phased array (VIPA), semiconductor mode-locked lasers (MLL), two-photon absorption (TPA), second-harmonic generation (SHG), and highly nonlinear fiber (HNLF), the spectrally encoded OCDMA is the most viable contender for the future fiber-to-the-home (FTTH) and data networks applications.

There is no doubt that the success of various OCDMAs depends upon the advancement of optical technology and devices, and on the ability to model them mathematically, in order to obtain their limits and their performance in a system. However, a

more important aspect in introducing successful OCDMA techniques or any other optical communication systems is essentially to introduce signal processing techniques that are fundamental to light behaviors and properties. It would be wrong to think that one can directly mimic concepts from radio and electronic-based communication systems and signal processing into optical communications and optical signal processing, since light and photonic devices could be categorically quite different from their electronic counterparts. It is essential first to understand the fundamental behaviors and characteristics of light and the optical devices to be used and subsequently to introduce signal processing techniques based upon the functionalities that are fundamental and natural to light and optics. It is for these reasons that OOCs and spectrally encoded OCDMA techniques proved to be so successful, since they are fundamental and natural to incoherent and coherent light properties and the optical signal processing techniques that follow them.

2. Advance Optical Orthogonal Codes Algorithms

OOCs defined by Salehi [6] and Chung *et al.* [8] are a family of (0,1) sequences with desired autocorrelation and cross-correlation properties providing asynchronous multiple-access communications with easy synchronization and good performance in OCDMA communication networks [6,7]. In this section we review a few of the most important algorithms in generating OOCs.

2.A. Mathematical Formulation

An optical orthogonal code $(n,w,\lambda_a,\lambda_c)$ is a family C of (0, 1) sequences of length n with constant Hamming weight w satisfying the following two properties.

1. Autocorrelation property. For any codeword $\mathbf{x}=(x_0,x_1,\ldots,x_{n-1})\in C$, the inequality $\Sigma_{i=0}^{n-1}x_i x_{i\oplus\tau}\leqslant\lambda_a$ holds for any integer $\tau\equiv 0(\mathrm{mod}\,n)$, and
2. Cross-correlation property. For any two distinct codewords $\mathbf{x},\mathbf{y}\in C$, the inequality $\Sigma_{i=0}^{n-1}x_i y_{i\oplus\tau}\leqslant\lambda_c$ holds for any integer τ,

where the notation $\oplus$ denotes the modulo-n addition [8]. When $\lambda_a=\lambda_c=\lambda$, we denote the OOC by (n,w,λ) for simplicity. The number of codewords is called the *size* of the OOC. From a practical point of view, a code with a large size is required [7]. To find the best possible codes, we need to determine an upper bound on the size of an OOC with the given parameters. Let $\Phi(n,w,\lambda_a,\lambda_c)$ be the largest possible size of an $(n,w,\lambda_a,\lambda_c)$ OOC. An OOC achieving this maximum size is said to be *optimal*. It is easily shown that if $w(w-1)>\lambda_a(n-1)$ then $\Phi(n,w,\lambda_a,\lambda_c)=0$ and if $w^2>\lambda_c n$ then $\Phi(n,w,\lambda_a,\lambda_c)\leqslant 1$ [14]. Based on the Johnson bound for constant-weight error correcting codes [15], we have the following bound [8]:

$$\Phi(n,w,\lambda)\leqslant\left\lfloor\frac{1}{w}\left\lfloor\frac{n-1}{w-1}\left\lfloor\frac{n-2}{w-2}\right\rfloor\cdots\left\lfloor\frac{n-\lambda+1}{w-\lambda+1}\left\lfloor\frac{n-\lambda}{w-\lambda}\right\rfloor\right\rfloor\cdots\right\rfloor\right\rfloor, \tag{1}$$

where the notation $\lfloor\ \rfloor$ denotes the integer floor function. Also, it is clear from the definition that $\Phi(n,w,\lambda_a,\lambda_c)\leqslant\Phi(n,w,\lambda)$ where $\lambda=\max\{\lambda_a,\lambda_c\}$. As an example, the following two sequences are the codewords of a (13, 3, 1) OOC [8]:

$$C=\{1100100000000,1010000100000\}. \tag{2}$$

This code is optimal since

$$\Phi(13,3,1)\leqslant\left\lfloor\frac{1}{3}\left\lfloor\frac{13-1}{3-1}\right\rfloor\right\rfloor=2.$$

Another useful depiction method for OOCs is the set-theoretical representation $X=\{k\in Z_n;x_k=1\}$ for each codeword $\mathbf{x}=(x_0,x_1,\ldots,x_{n-1})$, where $Z_n=\{0,1,\ldots,n-1\}$ denotes the modulo-n integers [8]. For example, the (40,4,1) OOC can be represented as

$$(40,4,1)-\mathrm{OOC}=\{\{0,1,28,37\},\{0,2,18,25\},\{0,5,11,19\}\}(\mathrm{mod}\,40). \tag{3}$$

Then the correlation properties for every codeword X and Y can be reformulated as follows:

$$\text{Autocorrelation property:} \quad |(a \oplus X) \cap (b \oplus X)| \leq \lambda_a$$

$$a \not\equiv b (\text{mod } n),$$

$$\text{Cross-correlation property:} \quad |(a \oplus X) \cap (b \oplus Y)| \leq \lambda_c,$$

where $a \oplus X$ is equal to $\{a \oplus x : x \in X\}$ and $|X|$ denotes the cardinality of the set X.

2.B. Construction Methods

There are several methods for constructing OOCs that can be categorized into two cases [8]. The first case includes direct methods that use mathematical structures such as projective geometry [8,16], finite field theory [14,17], and design theory [14,18–20]. The second case includes search methods that use computer algorithms such as greedy and accelerated greedy algorithms [8] and the outer-product matrix algorithm [21].

The first mathematical design method of OOCs, presented in the original paper on OOCs [8], is based on finite projective geometry. There is an $(n, w, 1)$ OOC corresponding to projective geometry $PG(d, q)$ where d is a positive integer and q is a prime power such that $n = (q^{d+1} - 1)/(q - 1)$ and $w = q + 1$. Each codeword corresponds to a line in $PG(d, q)$ where each line is obtained from a plane crossing the origin in a $(d+1)$-dimensional vector space on Galois field $GF(q)$. It was shown that [8] the number of codewords obtained from this method is equal to $(q^d - 1)/(q^2 - 1)$ for even d and $(q^d - q)/(q^2 - 1)$ when d is odd, which achieve the Johnson bound in each of the two cases. Therefore, this method gives an optimal $(n, w, 1)$ OOC. For example, the set-theoretical representation of optimal (341,5,1) OOC obtained from $PG(4, 2^2)$ with 17 codewords is given in Table 1 [8].

Due to the Johnson bound, OOCs with $\lambda = 1$ have a fewer number of codewords and therefore few users can be accommodated in the corresponding OCDMA networks. Hence, OOCs with $\lambda_a, \lambda_c > 1$, which have more codewords and are sometimes called generalized OOC, have been examined in OCDMA systems. Surprisingly, it was shown in [22], as an example, that for 50 users, the (1000,12,2) OOC has a better performance than (1000,5,1) OOC. This point has been deeply analyzed and verified in [23], and it was shown that OOCs with $\lambda = 2, 3$ could have better performance than codes with $\lambda = 1$. Consequently, the construction methods of generalized OOCs have found a special importance. The first construction method of OOCs with $\lambda = 2$ is due to Chung and Kumar [14], which uses finite field theory to design an optimal $(p^{2m} - 1, p^m + 1, 2)$ OOC with $p^m - 2$ codewords where p is a prime number and m is a positive integer. Let α be a primitive element of $GF(p^{2m})$ and $\beta = \alpha^{p^m+1}$, then the set-theoretical representation of codewords is as follows:

$$S_i = \{\log_\alpha(x); (x-1)^{p^m+1} = \beta^i\}, \quad i = 1, 2, \ldots, p^m - 2. \tag{4}$$

Table 1. Codewords of (341,5,1) OOC

S_1	0	1	85	21	5
S_2	0	2	170	10	42
S_3	0	3	111	104	53
S_4	0	6	222	106	208
S_5	0	9	268	151	105
S_6	0	11	45	76	198
S_7	0	12	103	75	212
S_8	0	13	305	227	43
S_9	0	15	107	146	164
S_{10}	0	17	264	203	165
S_{11}	0	19	88	267	220
S_{12}	0	22	90	55	152
S_{13}	0	23	293	252	118
S_{14}	0	24	206	83	150
S_{15}	0	25	54	169	221
S_{16}	0	26	269	86	113
S_{17}	0	37	147	217	81

Table 2 contains the codewords of (63,9,2) OOC obtained for $p=2$ and $m=3$ [14]. There is a strong relationship between OOCs and constant-weight cyclically permutable codes (CPCs). In other words, an (n,w,λ) OOC is equivalent to the $(n,2w-2\lambda,w)$ CPC, which indicates an error-correcting code of length n, weight w, and minimum Hamming distance $2w-2\lambda$. Every cyclic shift of CPC codeword is also a codeword [24]. So, using construction methods of CPCs we can design new OOCs. In [24] several such methods, especially for $\lambda=1$, have been examined.

OOCs with unequal autocorrelation and cross-correlation constraints were investigated in detail by Yang and Fuja [18]. A new upper bound useful for case $\lambda_a>\lambda_c$, presented in [18], is as follows:

$$\Phi(n,w,\lambda+m,\lambda)\leq\left\lfloor\frac{(\lambda+m)(n-1)(n-2)\cdots(n-\lambda)}{w(w-1)(w-2)\cdots(w-\lambda)}\right\rfloor. \tag{5}$$

For example, from the Johnson bound for (41,4,2,1) OOC we have $\Phi(41,4,2,1)\leq\Phi(41,4,2)\leq 63$ while from the above bound we have $\Phi(41,4,2,1)\leq 6$, which indicates that it is impossible to have more than six codewords for (41,4,2,1) OOC; so, for $\lambda_a>\lambda_c$ it is tighter than Johnson bound.

Another useful method for OOC design is presented in [17], which uses two mathematical structures; namely, perfect difference set (PDS) and finite Mobios geometry (MG). A k subset $D=\{d_1,d_2,\ldots,d_k\}$ of $Z_n=\{0,1,\ldots,n-1\}$ is called an (n,k,λ) PDS whenever for every $a\equiv 0(\mathrm{mod}\,n)$ there are exactly λ ordered pairs (d_i,d_j), $i\neq j$ such that $d_i-d_j\equiv a(\mathrm{mod}\,n)$. A finite Mobios geometry $MG(q,r)$ with prime power q and positive integer r is an extended Galois field $GF(q^r)\cup\{\infty\}$ with all circles on it. Based on a one-to-one correspondence between $(q^{2r}+q^r+1,q^r+1,1)$ PDS and $MG(q,r)$, an OOC with parameters $(q^{2r}+q^r+1,q+1,1,2)$ and size $2q^{r-1}[(q^{2r}-1)/(q^2-1)]$ can be obtained. As an example, if $q=2$ and $r=2$, we have a (21,3,1,2) OOC with 20 codewords [17]. The advantage of this method is in its ability to generate a large number of codewords, but the low weight requirement is a major drawback for this structure.

There are some recursive constructions for OOCs [8,25]. One of the best recursive methods for (n,w,λ) OOC design was obtained by Chu and Golomb [26]. This method uses r-simple matrices over a cyclic group for recursive construction of OOCs, which indicates that if there exists an (n,w,λ) OOC with T codewords, then there exists an (nm,w,λ) OOC with Tm^λ codewords whenever the prime factors of m are not less than w. As an example, for $m=11$ and (63,9,2) OOC with six codewords, this method constructs a (693,9,2) OOC with $6\times 11^2=726$ codewords [26]. One of the advantages of this method is that if the (n,w,λ) OOC is optimal then the constructed (nm,w,λ) OOC is at least asymptotically optimal [26].

Cyclotomic classes and numbers with respect to the finite field $GF(q)$ are the mathematical structures that can be used to construct OOCs. Using this method, Ding and Xing presented several classes of $(2^m-1,w,2)$ OOCs [27]. Also, five classes of $(q-1,w,2)$ OOCs where q is a power of odd prime have been derived using cyclotomy [28].

By using finite projective geometry, we can also design OOCs with $\lambda>1$. In [16], based on conics on finite projective planes in the projective geometry $PG(3,q)$, an asymptotically optimal $(q^3+q^2+q+1,q+1,2)$ OOC with q^3-q^2+q codewords has been obtained. For example, if $q=3$, the (40,4,2) OOC with 21 codewords is obtained [16].

The balanced incomplete block design (BIBD) is one of the most beautiful structures in discrete mathematics that has a close relation with OOCs. In other words, every (n,w,λ) OOC is equivalent to a $(\lambda+1)-(n,w,1)$ strictly cyclic partial design [25,20]. Since there are several methods for constructing the BIBD, such as those of Wilson [14,18,19] and Hanani, we can use them to design OOCs. Wilson's method is applied for designing of $(n,w,1)$ OOC [14] and $(n,w,2,1)$ OOC [18]. Both cases are

Table 2. Codewords of (63,9,2) OOC

S_1	{1,5,8,18,28,31,35,40,59}
S_2	{2,7,10,16,17,36,55,56,62}
S_3	{3,11,24,25,27,29,30,43,51}
S_4	{4,9,14,20,32,34,47,49,61}
S_5	{6,22,23,39,48,50,54,58,60}
S_6	{12,15,33,37,44,45,46,53,57}

categorized to even and odd w. In this method n is a prime number obtained from weight w and the size of the code. For example, the following optimal (37,5,2,1) OOC with three codewords have been obtained from Wilson's method for odd w:

$$(37,5,2,1) - \text{OOC} = \{\{0,1,6,31,36\},\{0,8,11,26,29\},\{0,10,14,23,27\}\} (\text{mod } 37). \quad (6)$$

Hanani's method [18,19] like Wilson's [14,18], is for the designing of $(n,w,1)$ OOC [19] and $(n,w,2,1)$ OOC [18]. This method for constructing $(n,w,1)$ OOC is categorized into two cases, namely, $w \equiv 2 \pmod 4$ and $w \equiv 3 \pmod 4$. But for the construction of $(n,w,2,1)$ OOC it is divided in two cases $w \equiv 0 \pmod 4$ and $w \equiv 1 \pmod 4$. In all these cases the code length n is a prime number obtained from the code weight and the number of codewords. The (41,4,2,1) OOC with the following five codewords are obtained from Hanani's method [18].

$$(41,4,2,1) - \text{OOC} = \{\{1,11,30,40\},\{12,16,25,29\},\{10,13,28,31\},\{3,4,37,38\},\{7,18,23,34\}\} (\text{mod } 41). \quad (7)$$

Although it seems that Hanani's method [18] is a special case of Wilson's construction [18], there are some code lengths that in Hanani's construction [19] yield codes while in Wilson's method they do not [19]. One of the best-known cases of BIBD is Steiner quadruple system (SQS). Based on SQS, Chu and Colbourn [20] suggested an algorithm for optimal $(n,4,2)$ OOC with $n \leqslant 44$. As an example, optimal (10,4,2) OOC with three codewords obtained from this method is as follows [20]:

$$(10,4,2) - \text{OOC} = \{\{0,2,4,7\},\{0,1,3,4\},\{0,1,2,6\}\} (\text{mod } 10). \quad (8)$$

2.C. Analysis and Design of OOCs using Matrix Algebra

For the last one-and-a-half decades, most approaches to OOC design were based on the initial inner-product definition of OOCs [6]. A major weakness of these approaches is that they can only support certain code lengths, code weights, and autocorrelation and cross-correlations integer values that have special properties. In other words, most algorithms developed so far cannot be easily extended to generalize for all integers of choice on code lengths, weights, and autocorrelation and cross-correlation constraints.

A whole new approach for the analysis and the design of OOCs based on the outer-product matrix was defined by Charmchi and Salehi [21]. For each codeword $\mathbf{x} = (x_0, x_1, \ldots, x_{n-1})$, its outer-product representation is defined as $D_{\mathbf{xx}} = \mathbf{x}^T\mathbf{x}$ and for two codewords $\mathbf{x}$ and $\mathbf{y}$, matrix $D_{\mathbf{xy}}$ is defined as $\mathbf{x}^T\mathbf{y}$. It was shown in [21] that the autocorrelation $\sum_{i=0}^{n-1} x_i x_{i\oplus\tau}$ is equal to the sum of the τ-diagonal of matrix $D_{\mathbf{xx}}$ and the cross correlation $\sum_{i=0}^{n-1} x_i y_{i\oplus\tau}$ is equal to the sum of the τ diagonal of matrix $D_{\mathbf{xy}}$. As an example, for (5,2,1) OOC with two codewords $\mathbf{x} = (1,0,1,0,0)$ and $\mathbf{y} = (1,1,0,0,0)$ the outer-product matrices $D_{\mathbf{xx}}$ and $D_{\mathbf{xy}}$ are as follows:

$$D_{\mathbf{xx}} = \begin{bmatrix} 1 & 0 & 1 & 0 & 0 \\ 0 & 0 & 0 & 0 & 0 \\ 1 & 0 & 1 & 0 & 0 \\ 0 & 0 & 0 & 0 & 0 \\ 0 & 0 & 0 & 0 & 0 \end{bmatrix}, \quad D_{\mathbf{xy}} = \begin{bmatrix} 1 & 1 & 0 & 0 & 0 \\ 0 & 0 & 0 & 0 & 0 \\ 1 & 1 & 0 & 0 & 0 \\ 0 & 0 & 0 & 0 & 0 \\ 0 & 0 & 0 & 0 & 0 \end{bmatrix}. \quad (9)$$

Based on outer-product matrices, a new definition of $(n,w,\lambda_a,1)$ OOC was presented in [21] that has tended to a matrix search algorithm for $(n,w,\lambda_a,1)$ OOC, with number of codewords that is closer to the Johnson bound than the greedy algorithm [21].

Outer-product representation of OOCs provides the possibility of using matrix algebra with rich literature in analyzing and designing OOCs. In other words, we can use matrix-based definitions of OOCs for algorithmic design of OOCs. Recently Alem [29] presented a full definition of $(n,w,\lambda_a,\lambda_c)$ OOC based on circulant matrices that establishes a mathematical structure on the space of all circulant matrices as a commuta-

tive algebra, which can be used to design new OOC construction algorithms. As an example, the circulant matrices of codewords $\mathbf{x}=(1,0,1,0,0)$ and $\mathbf{y}=(1,1,0,0,0)$ of (5,2,1) OOC are as follows:

$$A_{\mathbf{x}}=\begin{bmatrix}1&0&1&0&0\\0&1&0&1&0\\0&0&1&0&1\\1&0&0&1&0\\0&1&0&0&1\end{bmatrix},\quad A_{\mathbf{y}}=\begin{bmatrix}1&1&0&0&0\\0&1&1&0&0\\0&0&1&1&0\\0&0&0&1&1\\1&0&0&0&1\end{bmatrix}. \tag{10}$$

Using Eq. (10) then the autocorrelation matrix $C_{\mathbf{x}x}$ and cross-correlation matrix $C_{\mathbf{x}y}$ are obtained as $A_{\mathbf{x}}A_{\mathbf{x}}^T$ and $A_{\mathbf{y}}A_{\mathbf{x}}^T$, respectively. Also, based on the spectrum of circulant matrices, we can establish a partitioning on the space of constant-weight (0,1) sequences to reduce the complexity of correlations computations in search algorithms and suggest new design algorithms.

3. Optical CDMA via Optical Orthogonal Codes (Incoherent OCDMA)

3.A. Receiver Structures for Fiber-Optic CDMA Systems

Figure 1 shows a typical fiber-optic CDMA (FO-CDMA) communication network based on a star configuration consisting of N transmitter and receiver pairs. For each user, the information data source is followed by an optical encoder that maps each bit of the output information source to a very high rate optical sequence that is then coupled into the common channel via a passive star coupler. At the receiver end of a FO-CDMA system, the received optical pulse sequence would be compared to a stored replica of itself (matched filtering) and to a threshold level at the comparator, for the data recovery. In a CDMA communication system, multiple-access interference (MAI) is recognized as the dominant source of noise that limits the system capacity. Several designs for receiver structure are proposed to be used in typical OCDMA systems using OOC in order to improve the system performance and increase the capacity by mitigating the MAI effect. In this section I discuss a few well-known receiver structures developed for the past fifteen years for the single-user detection schemes.

The simplest structure, namely, the correlator receiver, includes a match filter, corresponding to its code pattern, and an integrate and dump circuit (Fig. 2). In FO-CDMA systems the match filter can be implemented by fiber tapped-delay lines at the receiver side. In [7] the correlator receiver for the detection of OOCs was proposed and analyzed. This receiver can be realized in the same all-optical tapped-delay line as the transmitter encoder. Delay lines in each branch serve to compensate for the corresponding delays induced at the encoder, which constitute the corresponding OOC. The properly delayed replicas add up to construct the output correlation signal, which is then fed to the photodetector, integrated, then dumped onto the thresholder electronic circuit. The major advantage of this system is that the limiting high-speed chip time decoding operation is done passively and optically.

If we denote the code length and the weight by L and w, respectively, and if each chip duration is equal to T_c, and if the positions of the pulsed mark chips corresponding to the code sequence are $c_1, c_2, \ldots$, and c_w, the optical match filter (passive optical tapped-delay line) consists of w fiber delay lines each of which make a delay equal to $(L-c_1)T_c$, $(L-c_2)T_c, \ldots$, and $(L-c_w)T_c$. Considering one bit duration, the output of the match filter, which is the combination of all w lines, the output signal has a peak at the time LT_c if the transmitted bit is ON. However, when the number of interfering

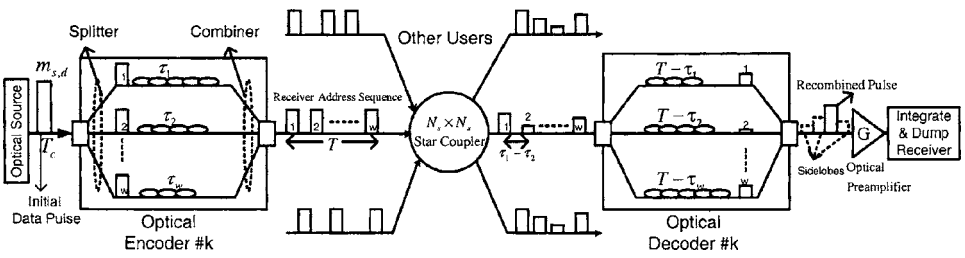

Fig. 1. Schematic of an OCDMA communication system with an all-optical encoder and decoder in star configuration.

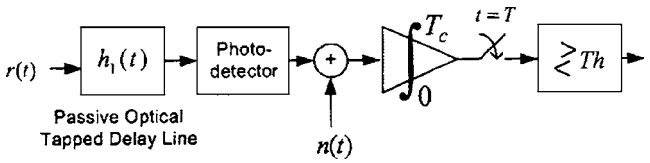

Fig. 2. Correlator receiver structure.

users is equal to or greater than w, we may observe such a peak in the absence of the desired user signal, i.e., the transmitted bit is OFF, and this causes an error.

Although the correlator receiver seems trivial, in the sense that it is an optimum receiver in the case of single user communication with no interference only, it can be much improved by taking into account other interfering users using some other OOC codes in the same fiber channel. In fact the first improvement was suggested by Salehi and Brackett [7]. The authors noted that in every definite chip time just that amount of intensity transmitted for a "1" bit may carry information, and any excess intensity is due to interference. Such an interfering term may cause a "0" data bit to be falsely decoded as 1. Thus an optical hard-limiter, which limits such excessive amounts of intensity, if placed before the conventional correlator receiver will block some interfering patterns from causing errors and improve the system performance. So they suggested employing an optical hard-limiter to suppress some interference patterns that are capable of producing errors and showed the improvement in system performance due to multiuser interference.

Performance improvement produced by a correlator+optical hard-limiter was not sufficient. Kwon [30] showed that an optical hard-limiter in a system using an avalanche photodiode (APD) only slightly improves the system performance. Later Ohtsuki *et al.* [31] and Ohtsuki [32] showed that adding another optical hard-limiter, this time after the optical correlator with a proper threshold setting for the second hard-limiter, results in a much better performance. In fact, such a configuration removes some interference pattern that could not be removed by the first hard-limiter. As a serious drawback for receivers incorporating an optical hard-limiter, such devices, though mathematically straightforward, are rather far from being mature and practical. They suffer from a nonideal transition range and show hysteresis. For this reason Shalaby introduced the concept of chip-level detection in OCDMA systems [33]. In this structure the decision is based upon the received power of each pulsed mark chip constituting the desired OOC instead of their combined power values as in the correlator receiver. In this structure the received power of each pulsed mark chip is compared with an optimum threshold. Bit 1 is decided if the power of all w pulsed chips is greater than the optimum threshold, otherwise 0 is decided. The results show a significant improvement in chip-level detection when compared to a simple correlator, especially when the number of interfering users increases.

There have been many efforts at obtaining optimum receiver structure in the area of direct-detection OCDMA systems. But the mathematical development for the case of the optimum receiver is not so promising since computational complexity prohibits any practical realization of such systems [34,35].

The correlator receiver in [7] is analyzed under an interference-limited assumption, while the more general analysis must take into account Poisson shot noise and photodetector dark current noise [22]. Both [34,35] consider shot noise and dark current in the context of a photon counting statistics framework. Finally, [30] assumes Gaussian statistics for the output signal of the photodetector incorporating all major sources of noise. A Gaussian approximation is a rather good approximation for the APD photodetector but is not so good for the conventional PIN diode detector, especially when the design is for low energy per bit systems.

Since thermal electronic noise is the dominant noise in many practical optical communication systems, there has been an actual demand for a general performance evaluation framework that not only considers Poisson distributed shot noise and dark current noise but also includes Gaussian distributed thermal noise along with a multiuser interference signal. Zahedi and Salehi [36] presented a unified model based on the photon counting technique that included practically all the above-mentioned sources of noise. With this approach general expressions for bit error rate (BER) for various receiver structures in FO-CDMA were obtained using meticulous and exact mathematical models. This work compares various receiver structures in rather real-

istic conditions and highlights that the correlator+double optical hard-limiter outperforms the chip-level detector when the transmitted energy per bit is low. As the power increases they both converge to the optimum single-user receiver as was shown by Shalaby [33]. On the other hand, the chip-level detector causes a significant improvement as compared with conventional correlator in medium to high power region, and the addition of a single optical hard-limiter prior to chip-level detection does not improve the system performance much.

Zahedi and Salehi [36] differentiated between the passive tapped-delay line correlator and the active correlator. It is assumed that for the passive tapped-delay line correlator the electronic circuit necessary is designed to perform a short-term integration (over a chip time), and for the active correlator the integration is on the whole bit period and hence is a much slower integrator. Results of this research show that, though requiring faster electronics, the passive correlator performs better in the thermal noise limited region. It is plausible because chip time integration means gathering less circuit noise than bit time integration. Figure 3 presents the performance of different passive and active structures of the studied receivers by showing the dependence of BER on the mean number of photons per chip. In this figure the typical values for the thermal noise and the dark current noise have been assumed. It has been observed that the effect of circuit noise on the performance of the chip-level receiver (Figure 3, curve *h*) is quite severe. The effectiveness of the optical hard-limiter in reducing the interference patterns can be observed from curves *a*, *b*, and *c*. However we do not reach an error-free communication system by increasing transmitted power, this is a consequence of the presence of MAI.

Finally in [37] Shalaby claims that while the correlator+double optical hard-limiter has a slight advantage over the chip-level detection scheme, the former requires high hardware complexity, hence is not practical.

3.B. Optical and Logic Gate-Based Receiver with Generalized OOC

Considering the mutual interference among multiple users the most desirable ON–OFF signature sequences are OOCs with autocorrelation and cross-correlation values equal to 1 ($\lambda=1$). However these families of codes may suffer from low cardinality in certain applications. In fact, although OOCs with $\lambda=1$ minimize the mutual interference between the users these codes are not necessarily the optimum codes in order to maximize the throughput of a typical OCDMA system. Furthermore Azizoglu *et al.* [22] showed that for the same number of users and the same code weight, the performance of OOCs with $\lambda=2$ may improve on the performance of strict OOCs ($\lambda=1$). This is because in the former case the code weight can be larger than strict OOCs and this can compensate for the effect of multiuser interference. Furthermore with λ

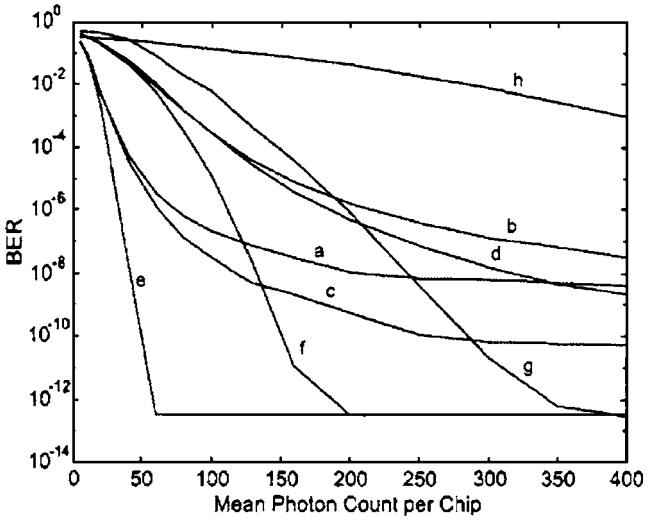

Fig. 3. Dependence of BER on mean photon count per chip for (a) passive correlator structure, (b) active correlator structure, (c) hardlimiter+passive correlator structure, (d) hardlimiter+active correlator structure, (e) double optical hardlimiter+passive correlator structure, (f) double optical hardlimiter+active correlator structure, (g) high-speed chip-level detector, and (h) optical chip-level detector.

=2 the OOC sets have a cardinality as high as a 100 to 1000 times bigger than strict OOCs. Also in [37] it was shown that using OOCs with $\lambda=2$ the throughput capacity of the system increases considerably for both correlation and chip-level receivers. By applying the Markov chain model Chen and Yang [38] obtained the exact expressions for the bit-error probability for arbitrary λ with a hard-limiting receiver for prime sequences.

Mashhadi and Salehi [23] obtained a simple solution on the performance of OCDMA systems with the optical AND logic gate as the receiver structure (Fig. 4), using generalized OOCs, i.e., arbitrary λ. They obtained the best codes for different design scenarios in an OCDMA system [23]. Furthermore, they showed that for most practical purposes OOCs with $1\leqslant\lambda\leqslant3$ achieve the best performance and they found the corresponding optimum weight that meets the best performance.

The most important result deduced from the exact solution is a set of empirical formulas that interrelate five important parameters; namely, minimum error rate, $P_{e,\min}$; minimum code length required, $L_{\min}$; maximum number of users, $N_{\max}$; optimum weight, w_{opt}; and optimum cross-correlation value λ_{opt}. From the solution and numerical results, it was shown that OOCs with $\lambda=2,3$ are more desirable than OOCs with $\lambda=1$, thereby giving a strong hint into the importance of constructing and generating OOCs with $\lambda=2,3$.

Finally we describe a technique introduced by Forouzan, *et al.* [39], namely, frame time hopping OCDMA (FTH-OCDMA) in which the orthogonality between code sequences is more relaxed. The FTH-OCDMA transmission method is an extension of a recently proposed technique based on an ultrawide-bandwidth radio communication scheme [40]. In this method each bit duration is divided into w frames each of which has a pulsed mark chip. The position of the pulsed mark chip of each frame is arbitrary. Thus if we denote the number of chips per bit by L, then the number of possible code sequences can be as high as $(L/w)^w$. This large cardinality makes this method interesting for certain applications. For instance, since the search space of FTH code sequences is very large this method is suitable for secure transmission of data in the physical layer. However since the cross-correlation coefficient of each two codes in FTH is not bound by an integer number smaller than w, on average we can say that the performance of FTH-OCDMA is always worse than the OCDMA system using generalized OOC, with $1\leqslant\lambda<w$, for the same number of users and the same code weight.

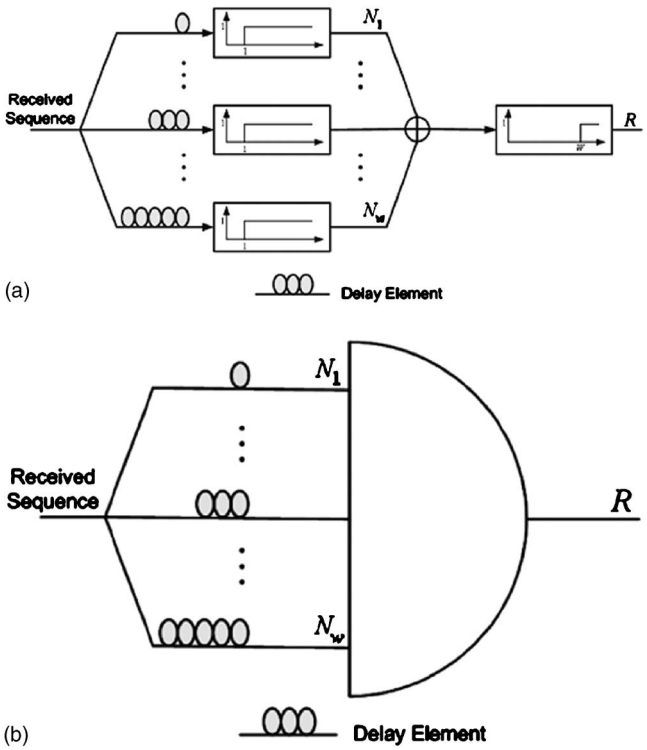

Fig. 4. (a) Ideal optical AND logic gate receiver structure for all-optical code recognition. (b) Equivalent functional AND logic gate receiver structure.

3.C. Architectural Consideration of Multiple Optical Amplifiers in OCDMA

Referring to Fig. 5 for a typical all-optical CDMA in a star topology using passive optical devices in conjunction with fiber-optic delay elements for encoding and decoding, one can observe the unavoidable attenuation in the initial transmitted pulse power due to the splitting of the pulse at the encoder, the star coupler, and the decoder. There are various ways to somewhat remedy this weakening effect on the pulse, such as the use of APDs [30,41–43] or optical preamplifiers at the receiver [44–48]. Unfortunately, none of the above amplifying methods can compensate for the degradation of optical signal-to-noise ratio (OSNR) that occurs in the intermediate stages of the network. Therefore, a much-preferred solution is to use optical amplifiers before all attenuating components similar to a postamplification configuration. In this scheme, due to the low noise figure of the optical amplifier, we can preserve the OSNR without imposing a severe power penalty. However, considering the saturation effect in optical amplifiers and the restrictions on the amount of launched power imposed by fiber nonlinearities, it can be foreseen that using a single postamplifier may not afford the required amount of signal gain. This, however, does suggest employing a configuration based on multiple optical amplifiers as described in detail by Razavi and Salehi [44,48].

From Fig. 5, due to the various stages of splitting in an all-optical CDMA system, it is not obvious how to decide on the number of optical amplifiers needed and, similarly, how to arrange or architect multiple amplifiers in a given system in order to obtain the best possible performance as a function of key system parameters. While in wavelength division multiple-access networks the limiting factor for utilizing optical amplifiers is their limited bandwidth and uniformity in frequency response, the performance of an FO-CDMA network using optical amplifiers is limited, primarily by quantum fluctuations in the received pulse photon number [44–47]. This fact requires us to use a photon counting approach in order to gain some insight into the optimum or suboptimum number of required amplifiers, their distribution architecture, and their respective gain setting parameters. To this end, in [44,48] the authors employ the statistical approach to obtain the related input–output characteristic functions for the number of photons in the address or signature pulse sequence codes at various stages of the network. The need for employing such a surgical and exhaustive method for performance analysis of an FO-CDMA network can further be illustrated by the following example.

Consider a Poisson-distributed pulse which, after traversing through the network, contains only ten photons on the average. This pulse with such a low OSNR can be amplified through a travelingwave optical amplifier to obtain a Laguerre distributed pulse with as many as 10,000 photons on the average. The corresponding output pulse power may be considered strong enough to overcome receiver noises such as thermal noise and dark current. However, from the statistical point of view, the content of shot noise (the randomness in the photon number) in this pulse is as large as that of a Poisson-distributed pulse with at most five photons on the average. This comes from the well-known 3 dB conventional noise figure associated with optical amplifiers.

From the above example, two main conclusions can be drawn. First, despite high-power pulses at the output of an optical amplifier, its corresponding OSNR value can be very low; therefore, the common assumption of Poisson distribution for the photon number in the received signal is completely violated for this case. Second, for a network that utilizes multiple optical amplifiers, the statistical variation of a photon number in a pulse traversing through the network must be considered from the beginning to the end of the network. In these networks, the corresponding OSNR at the receiver side is a function of the initial OSNR and cannot be predicted easily without considering the effect of all the components that comprise a network.

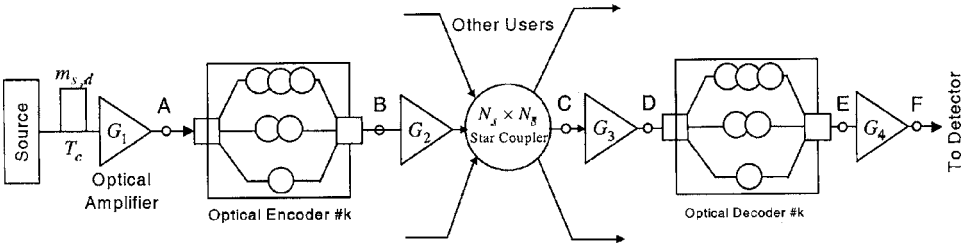

Fig. 5. FO-CDMA network incorporating multiple optical amplifiers.

Based on the analysis developed in [48] the authors obtain the compounded characteristic function at the output of the receiver photodetector considering shot noise, background noise due to extinction power of the sources, and thermal noise due to electronic circuitry. For the system analysis, they assume intensity modulation–direct detection with ON–OFF Keying (OOK) signaling. The BER computation was performed using two methods; namely, saddle-point and Gaussian approximations. They use BER results to explore the dependence of the system performance on the number and the position of optical amplifiers, as a function of code weight, bit rate, the number of amplified spontaneous emission (ASE) noise modes, and the number of users.

We summarize the results of [48] in Fig. 6, which represents the minimum probability of error for different optical amplifier configurations versus input photon number, neglecting path attenuation effect. The gains labeled on each curve show the amplifiers that have been used in that configuration. These configurations can be partitioned into three groups according to the number of amplifiers used. Assuming perfect splitting and combining, it is not advantageous to use both the third and fourth amplifiers, since the main user's recombined pulse has the same power as each of the pulses in the main user's pulse sequence before decoding. Therefore, if the output mean photon number after the third amplifier meets the amplifier saturation criterion, then it is also the case for the decoder output after recombination. Moreover, the results show that in all cases where we have used the third amplifier instead of the fourth amplifier, we obtain a better performance.

A major point that must be considered to justify Fig. 6 is that every attenuation effect on a single pulse decreases the inherent OSNR corresponding to that pulse. The OSNR reduction cannot be compensated for by amplification, since the amplifiers have a noise figure greater than 1 [49]. So, for those configurations that have a great distance and therefore a great attenuation between two successive amplifications, the performance will be degraded. For example, in Fig. 13(b), the performance of the configuration (G_1,G_4) is worse than that of configurations (G_2,G_3) and (G_1,G_3). On the other hand, a system with three successive amplifiers placed at the first, second, and the third positions yields the best performance among other configurations. This is completely reasonable, since this configuration avoids the OSNR degradation as much as possible, and, further, the postamplification criterion is inherently considered in this case. Finally, it should be noted that none of the configurations lead to error-free performance, since the BER floor is the consequence of the presence of the MAI.

3.D. OOC-Based Synchronization in OCDMA

In all CDMA systems to extract data bits from the spread stream of pulses, which constitutes the desired signature code properly, the receiver needs to know the correct reference time of the specified code pattern that carries the desired information bit [50–52]. Similar to the wireless CDMA systems, OCDMA systems' synchronization circuit consists of two stages, namely, acquisition and tracking blocks, as is shown in Fig. 7. In the acquisition stage the receiver is synchronized with its corresponding code with an accuracy that is better than or equal to half of the chip duration in the start-up phase. The exact and dynamic synchronization is achieved during the tracking stage.

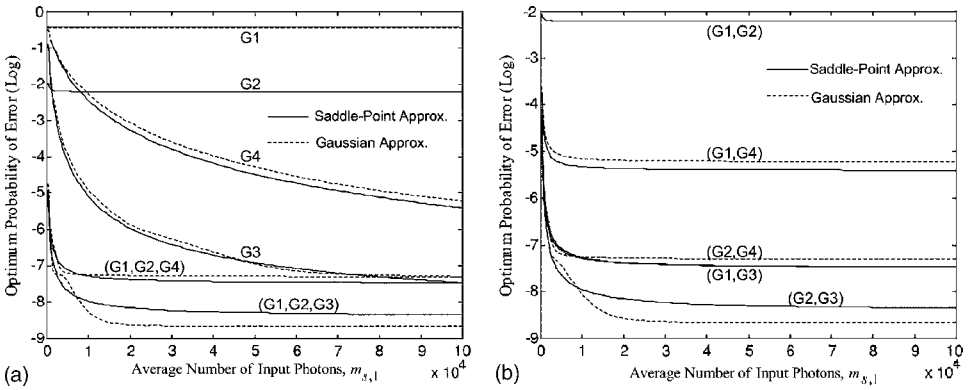

Fig. 6. BER versus initial OSNR, using different configurations for amplifiers.

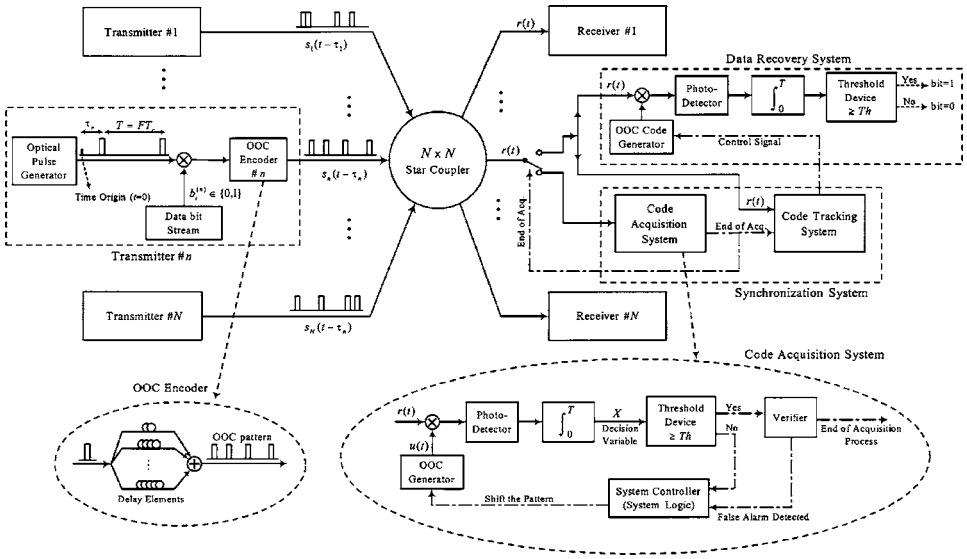

Fig. 7. OOC-CDMA network, synchronization operation.

In evaluating the performance of OCDMA systems, the majority of mentioned works in Subsection 2.A assume perfect synchronization between each receiver and transmitter pair. However, Yang [53] considered a simple synchronization method for noncoherent OCDMA and highlighted the importance of synchronization by showing the degradation in the performance of the system when the synchronization between the receiver and transmitter is not ideal.

Later Mustapha and Ormondroyd [54] introduced a serial-search synchronizer and a dual threshold sequential method [55] for synchronization of an OOC-based OCDMA system. They also investigated the effect of MAI on the acquisition performance of a sequential detection acquisition system [56], and showed that the optimum threshold of the acquisition block depends on the number of active interfering users. Keshavarzian and Salehi [57] analyze the performance of the simple serial-search algorithm for an OCDMA system using OOC codes. In this approach, assuming chip synchronicity, the receiver encounters an ambiguity equal to L cells each corresponding to one possible cyclic shift of the targeted OOC code. In the simple serial-search algorithm one cell is randomly selected and it is assumed to be the correct cell. A correlation between the received data and the selected code over a bit time duration is obtained. If the output of the correlation is greater than the optimum threshold, then the first randomly selected cell is the correct cell. Otherwise, we examine the next cell. So by continuing this algorithm, and in maximum L stages, we obtain the correct cell in the ideal case. The Markov chain model simplifies the analysis of various acquisition algorithms. Such a model is depicted in Fig. 8 for the so-called simple serial-search model. Each cell is represented by a node. Here we assume that the Lth node is the node representing the correct shift. P_D is the probability of correct detection. Transmission between each two cells is represented by a transfer function with parameter z. The power of z indicates delay in bit duration. So we observe that the transfer function of the correct decision on the correct cell is $P_D z$ and the incorrect decision is $(1-P_D)z$. P_D is not equal to 1 in the real case due to the shot noise effect. The transfer function between each two incorrect cells is defined as $H(z)$. Also we denote the false alarm probability by P_{FA}. When correlation on an incorrect shift exceeds optimum threshold a false alarm occurs;. P_{FA} is not equal to zero because of MAI and environmental noise effects. In Fig. 8, D indicates the time that the tracking circuit requires in recognizing the false decision in an acquisition block. If $U(z)$ indicates the transfer function of the above chain to the correct node, by averaging over the probability of starting with any node, it is shown that $U(z)$ is the moment generating function (MGF) of the mean acquisition time [56–58]. Hence the mean of acquisition time is obtained by $\{[dU(z)]/dz\}|_{z=1}$.

In [57] it was shown that the mean time required for simple serial-search synchronization is of the order of half code length. In this comprehensive study, major sources of noise i.e., MAI, shot noise, and dark current were considered. They concluded that

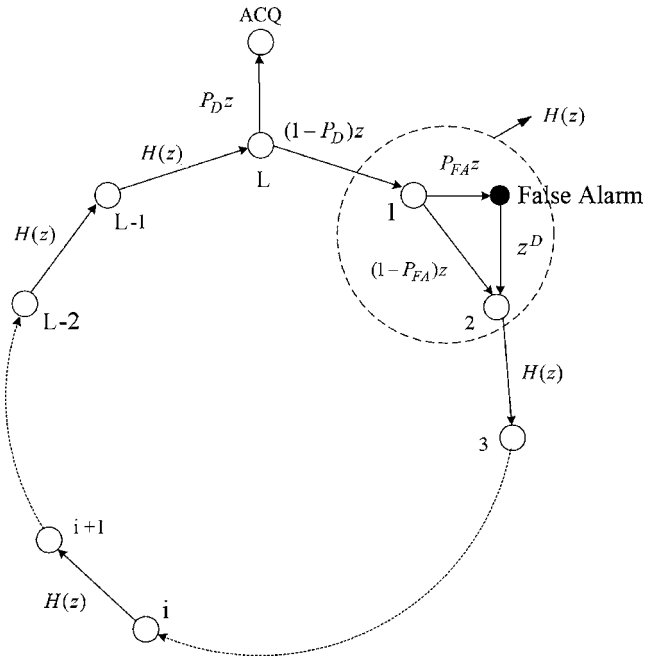

Fig. 8. Markov chain model for simple serial-search algorithm.

in a typical system, the shot noise effect can be neglected in analyzing the performance of the synchronization system.

The critical parameter for each synchronization algorithm is the acquisition mean time. It is evident that the less mean time of acquisition the more efficient the algorithm in use will be. In [58] the authors introduce and analyze a novel algorithm; namely, a multiple-shift algorithm to reduce the mean time of acquisition process. In this method, if we have L ambiguity cells. To find the correct cell we divide L cells into Q groups, each of which contain L/Q cells. In the first stage we find out the correct group that contains the correct cell by serial search on the groups, and in the second stage our search space is just on the correct group and a serial search is performed to find the correct cell. Therefore, roughly speaking, we can predict that the average time of acquisition is related to $(Q/2)+(L/2Q)$. By choosing $Q=\sqrt{L}$ the mean time of acquisition will be of the order of $\sqrt{L}$, which is much smaller than $L/2$ due to simple serial search average time, especially for large values of L. Figure 9 shows the Markov diagram for the multiple-shift method. Assuming that the Qth group contains the correct cell then $H(z)$ and $h(z)$ are the transfer functions between two incorrect nodes in the first and the second stage, respectively. Assuming that we have found the correct group then, similar to the simple serial-search method, an initial random phase v is selected. The other transfer functions that are needed to describe the multiple-shift method are $H_{\text{det}}(z)$ and $H_{\text{miss}}(z)$, the former being the transfer function from node Q to acquisition state and the latter being the transfer function from node Q to node 1. To obtain the exact value of mean acquisition time we must compute the transfer function $U(z)$ due to the Markov chain of Fig. 9. The multiple-shift algorithm is actually an efficient serial-search method that can be regarded as a variation of a binary search method and therefore can be used in many other applications other than code acquisition.

The tracking circuit performs important roles in a communication system and also in a typical OCDMA system. In general the received code from the acquisition block has an ambiguity in phase that is less than $T_c/2$. The main task of the tracking circuit is in minimizing this ambiguity. Ghaffari *et al.* [59] analyzed the effect of tracking block noise on the performance of a typical wireless OCDMA LAN.

3.E. Advanced Block-Coded PPM Signaling for OCDMA

With the advent of FO-CDMA technology, a large body of research work has been carried out around finding powerful code structures and effective signalings that can enhance such a system's capacity and performance. Among the possible signalings for

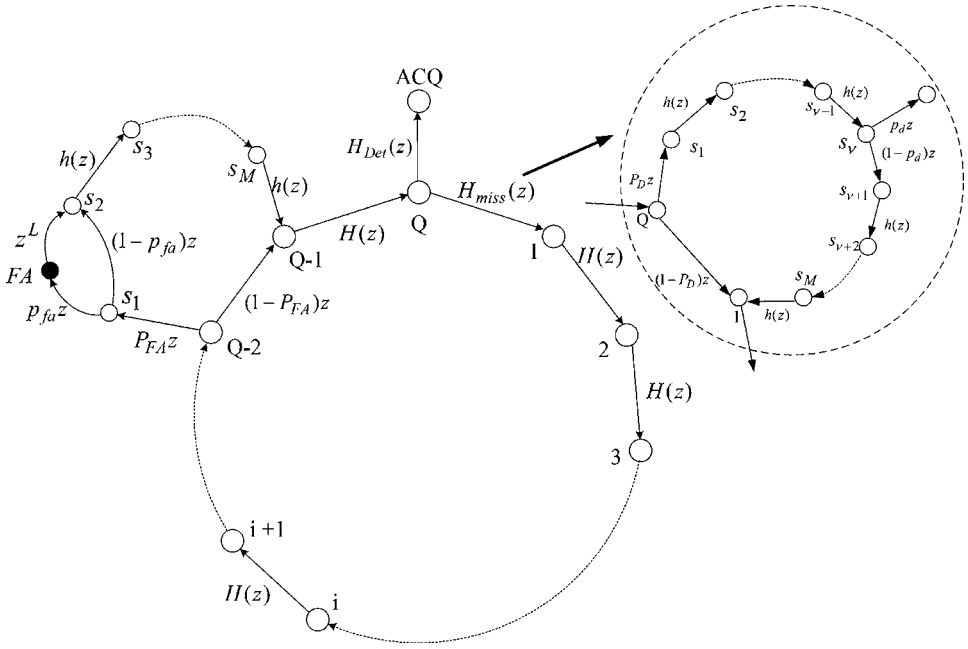

Fig. 9. Markov chain model for multiple-shift algorithm.

an optical communication system, OOK has been studied more than other signalings due to its simple operation and ease of analysis.

In OOK information bit 1 is transmitted by an *ON* optical pulse and information bit 0 is transmitted by an *OFF* pulse. So in optical systems, using OOK as the signaling format, the receiver must obtain an optimum threshold to decide on the transmitted information bit. In many conditions it is shown that probability of error strongly depends on the threshold value and threshold strongly varies with variations in input photons and environmental parameters. This implies that if the receiver has no accurate information on the variation of system noise, the probability of error obtained is erroneous.

On the other hand pulse position modulation (PPM) signaling is an alternative to OOK in many optical communications systems. In the PPM signaling format each symbol is represented by the position of the optical pulse among M possible time slots. If the time slots are disjoint we call this type of PPM as M-ary PPM signaling (Fig. 10). One can check easily that if the available bandwidth of the system is constant, the throughput offered by M-ary PPM is less than the OOK by a factor of $\log M/M$. On the other hand it is shown that M-ary PPM is much more energy efficient than the OOK signaling.

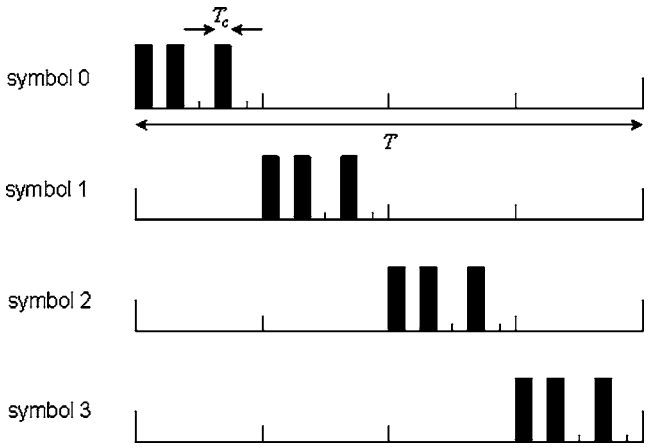

Fig. 10. Example of the transmitted signal formats of a single user in a PPM-CDMA system with $M=4$, $L=8$, and $w=3$.

However, performance analysis of M-ary PPM for OCDMA systems has been the subject of interest [41,60,61]. In the most standard form of optical PPM-CDMA systems, each user produces equiprobable M-ary data symbols. Each symbol modulates the position of a laser pulse with a temporal width that is equal to $1/M$ of the whole symbol duration. The modulated laser pulse is then spread within the time slot to generate the optical PPM-CDMA pulse sequence. In other words, each user's symbol interval is divided into M slots where each slot contains the corresponding spreading code. To send the mth symbol the spreading code of the corresponding user is placed in the mth time slot and the other time slots remain *OFF*. Therefore for PPM signaling, the optimum receiver is just a comparator between M received signal photons from M separate time slots and consequently there is no need to compute an optimum threshold, which results in simplifying the receiver structure.

It has been shown that for an M-ary PPM optical communication system the more the signaling multiplicative parameter, i.e., M, the less the system throughput. On the other hand in a typical M-ary PPM OCDMA system MAI is reduced by increasing signaling multiplicative parameter M. So there is a trade-off between the spectral inefficiency and MAI reduction that will determine the proper value of the multiplicative parameter of the signaling.

However it can be shown that when we deal with generalized OOC ($\lambda \geqslant 1$) as the signature sequence in M-ary PPM signaling, system throughput outperforms the OOK-OCDMA systems. As a result in this method we not only have the desired feature of M-ary PPM, i.e., energy efficiency, but also mitigate bandwidth inefficiency considerably.

To improve the throughput efficiency of M-ary PPM, overlapping PPM (OPPM) is an interesting alternative. In this method the positions of different symbols are not necessarily disjoint as is shown in Fig. 11. This type of signaling can be considered as a generalization to PPM where overlapping is allowed between pulse positions. OPPM retains some advantages of M-ary PPM, such as simplicity of implementation. It also improves the system's throughput without the need to decrease the pulse width. In [62,63] Shalaby suggests employing OPPM in OCDMA systems and shows that this signaling improves performance and throughput of the system when compared to OOK and M-ary PPM signalings. Although when the overlapping index increases the need for accurate synchronization will be more critical.

In [64] the authors have presented a novel encoder and decoder architecture for an M-ary OCDMA system using PPM. They demonstrated that the switched modulator reduces the transmitter complexity while the all-optical demodulator eliminates the need for expensive and complex electronics at the receiver end. Another experimental setup for a 2D M-ary PPM is presented in [65], where the authors have used a phase maintenance (PM) combiner to reduce system losses as well as reducing optical beat interference (OBI).

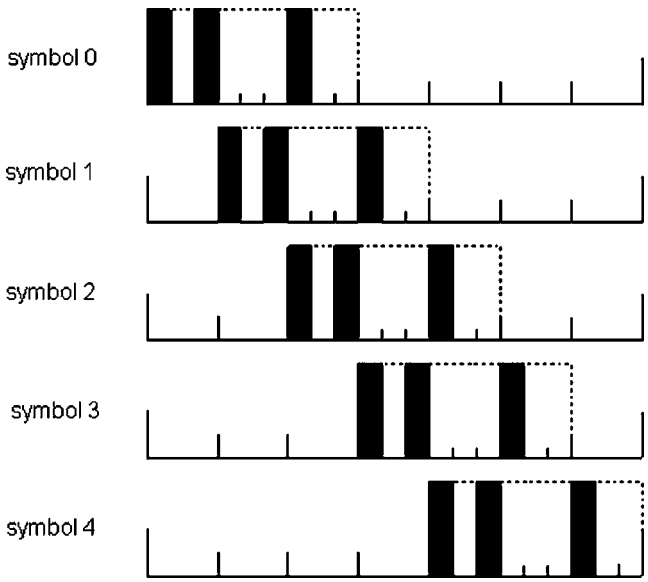

Fig. 11. Example of the transmitted signal formats of single user in an OPPM-CDMA system with $M=5$, $L=9$, and $w=3$.

3.F. 2-D OCDMA

In general, CDMA is relatively poor in terms of spectral efficiency resulting in low throughputs. It is shown that using (2D) optical CDMA can improve the overall network throughput. Vannucci [66] proposed a hybrid scheme to combine WDM and CDMA in such a way that the superior features of each technique mitigate the shortcomings of the other. It was shown that using different wavelengths improves spectral efficiency of OCDMA and using OCDMA greatly releases frequency control requirements. Tancevski and Andonovic [67] proposed a 2D time spreading integrated with a wavelength hopping pattern. By using prime codes in both time and wavelength dimensions the authors showed that the constructed codes have an autocorrelation function with zero sidelobes and a cross-correlation of at most one, and thus improve the orthogonality condition when compared to 1D prime sequences. Yang and Kwong [68] did an in-depth analysis in order to obtain the performance of a hybrid wavelength division multiple access (WDMA)+CDMA and some construction algorithms were presented for 2-D codes or the multiwavelength CDMA scheme. The authors showed that the multiwavelength CDMA outperforms the hybrid scheme under some conditions.

In general a family of 2D OOC codes can be represented by five important parameters $(N\times M, w, \lambda_a, \lambda_c)$, where N is the code length in time domain, M is the number of available wavelengths, w represents code weight, and λ_a and λ_c correspond to autocorrelation and cross-correlation values, respectively (Fig. 12). The above 2D family of OOC codes increases the cardinality with a smaller, if any, reduction in the user's data rate, and surely at the expense of increased transmitter and receiver complexity. As in typical time-spreading (1D) incoherent OCDMA systems, each user's data stream is encoded by its corresponding 2D code. The only difference being that in the 2D coding scheme, each marked or pulsed chip is transmitted via a different wavelength or center frequency. These wavelengths are chosen from a set of available wavelengths and the process of wavelength selection depends explicitly on the particular code structure, which itself depends on the correlation constraints of the 2D code family in use.

Nevertheless, expanding 1D codes to proper 2D codes is a problem that has attracted much effort and interest. Shivaleela *et al.* [69] designed a code family with single-pulse-per-row and desired properties. Such codes are very convenient especially for space–time 2D implementations. They also proposed [70] a new family of codes for wavelength–time 2D systems using multiple-pulse-per-row minimizing autocorrelation and cross correlation of code members. Yim *et al.* [71] discusses search algorithms and some trade-offs for constructing 2D codes with unit correlations. They have also studied [72] codes devised for OCDMA with differential detection that must fulfill different requirements.

Fathallah *et al.* [73] suggest using the FBG to implement a 2D fast frequency hopped (FFH) OCDMA scheme on an all-optical platform achieving very high bit rates. A broadband optical signal from an incoherent optical source is incident upon the FBG array devices. Thus the power spectrum of the transmitted signals for marked or pulsed chips depends on both the spectrum of the broadband light and field domain impulse response of the FBG array device (Fig. 13). They show that their pro-

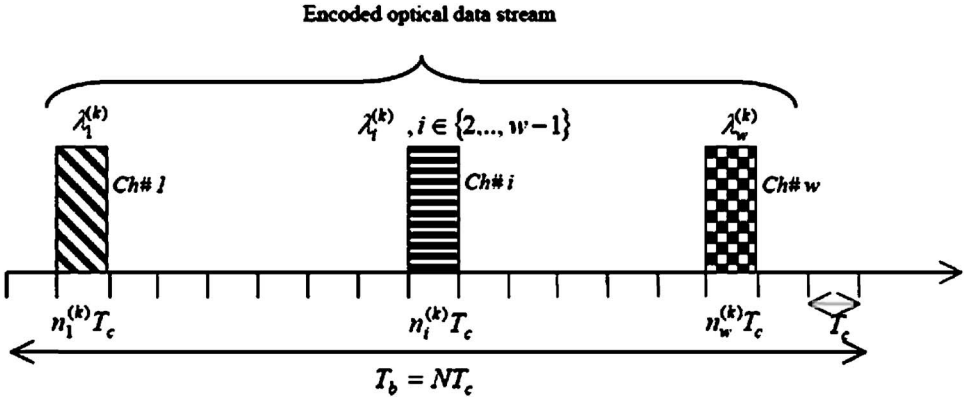

Fig. 12. Encoded pulses of 2D OCDMA system.

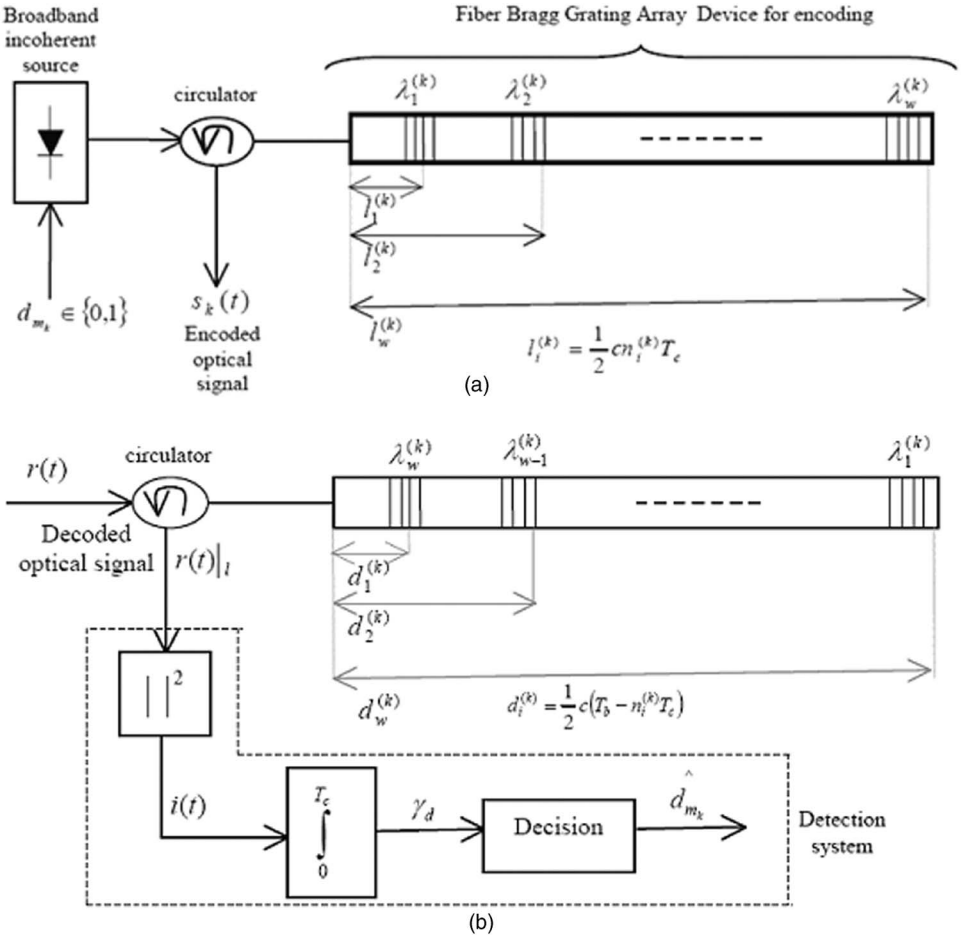

Fig. 13. (a) Encoding and (b) decoding structure based on FBG arrays.

posed scheme offers a large number of simultaneous users' codes with low-cross-talk and it outperforms 1D OCDMA for a given code length using a correlator receiver.

Many other published works relating construction of 2D code matrices and evaluation of the system performance can be found in the literature [74–78]. Among them we highlight papers by research groups at USC, such as Mendez *et al.* [74,77] and Saghari *et al.* [78], and at Hofstra University led by Kwong *et al.* [75]. Also, examples of 3-D codes are given in [79], using wavelength, space and time for defining the codes; and in [80,81], using wavelength, polarization, and time for the same purpose.

In practice various sources of noise do affect the performance of an incoherent OCDMA system. Among them phase induced intensity noise and beat noise can be considerable [82–84]. From the above references it can be concluded that the beat noise can in general degrade the performance of coherent time-spreading OCDMA systems [82], while in incoherent OCDMA systems, MAI is the dominant noise and the effect of beat noise is minimal [82].

4. Coherent Spectrally Encoded Ultrashort Light Pulse CDMA

Coding in OCDMA techniques incorporating coherent ultrashort light pulses can be either in frequency domain or time domain. In both schemes the result of the encoding is a pseudorandom light burst whose autocorrelation is a peaked ultrashort pulse and its cross correlation with waveforms generated with different codes remain a low intensity noiselike signal. In the following we first briefly describe the main representative technique of each scheme along with different approaches that have been used to implement the related encoder–decoder (E/D). Then, the most contentious part of the receiver, i.e., the optical thresholder (or the ultrashort pulse detector), is discussed and methods that have so far been used for its realization are reviewed.

4.A. Spectrally Phase Encoded OCDMA

In this technique, which was first introduced by Salehi *et al.* [13], the pseudorandom code assigned to each user is applied directly to the spectrum of the light pulse in the transmitter. The 4F arrangement in Fig. 14, which was first used to implement the technique, best illustrates the main idea [13]. The first grating spatially decomposes the spectral components of the incident light pulse (which represents a binary 1) and then they are mapped to the focal plane of the first lens, where they pass through a mask that modifies their phase according to a pseudorandom code. The modified spectrum is then collapsed by the second lens and the second grating back into a single optical beam. As a result of the spectrum slicing induced by the phase mask, the pulse spreads in time and becomes a low intensity pseudonoise light burst [13].

A receiver of this technique consists of a decoder and an optical threshold device. The optical decoder is similar to the optical encoder except that its phase mask is the complex conjugate of the encoding mask. Thus a pulse is properly decoded when the encoding and decoding masks are a complex conjugate pair. In this case the spectral phase shifts are removed and the original coherent ultrashort light pulse is reconstructed. On the other hand, when the encoding and decoding masks do not match, the spectral phase shifts are rearranged but not removed, and the pulse at the output of the decoder remains a low intensity pseudonoise burst. The threshold device is set to detect data corresponding to intense, properly decoded pulses and to reject low intensity, improperly decoded, pseudonoise bursts.

4.A.1. Enabling Technologies for Spectral Phase Encoder–Decoder

Besides the above 4F (diffraction) grating pair setup, which uses large free-space bulk optics and also suffers from inadequate resolution for long code lengths, some other methods have been proposed for the implementation of the spectral phase E/D. In the following we describe these methods and the related experimental results.

VIPA. A new structure called VIPA [85], was adopted to replace the grating part of the conventional 4F structure to increase its spectral resolution by Etemad *et al.* [86]. VIPA is essentially an optical disperser and consists of a collimator, a glass plate, and a set of focusing lenses. The glass plate is coated on one side to be perfectly reflective and on another side to be partially transmittive and has a small angle with respect to optical axis. The optical collimated beam enters the plate from an uncoated window and gets trapped between the two opposite sides of the plate. In each roundtrip some ratio of beam escapes. Each escaped beam seems to be originated from a virtual independent point source with some phase delay, giving the apparatus its name. By getting far from the plate, these escaped phase-delayed beams interfere and by virtue of the well-known concept behind gratings the spectral content of optical beam gets dispersed. Focusing lenses serve to translate angular dispersion to spatial resolution. In an OCDMA experiment using VIPA [86], a spectral phase coding with a resolution of ~1 GHz was achieved (Fig. 15). More compact solutions using other kinds of gratings such as FBGs and AWGs were proposed by Grunet-Jepsen *et al.* [87] and Tsuda *et al.* [88].

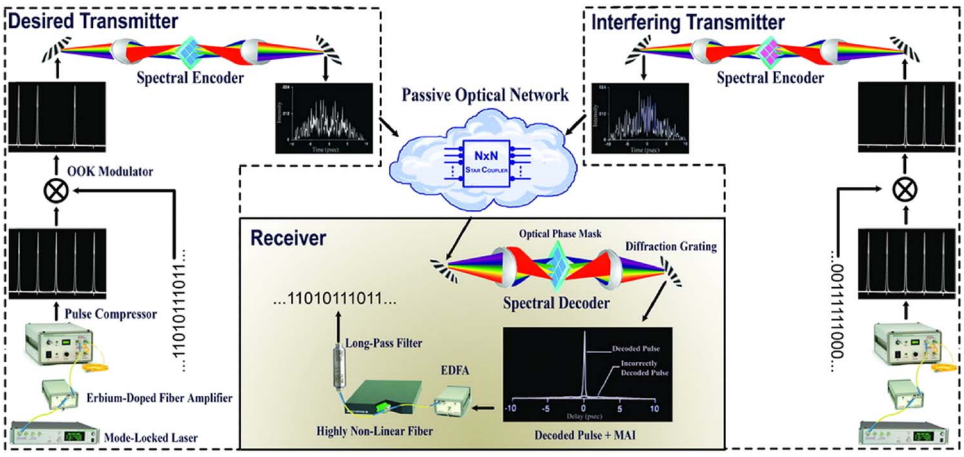

Fig. 14. Proposed scheme for optical CDMA based on spectral encoding and decoding of ultrashort light pulses.

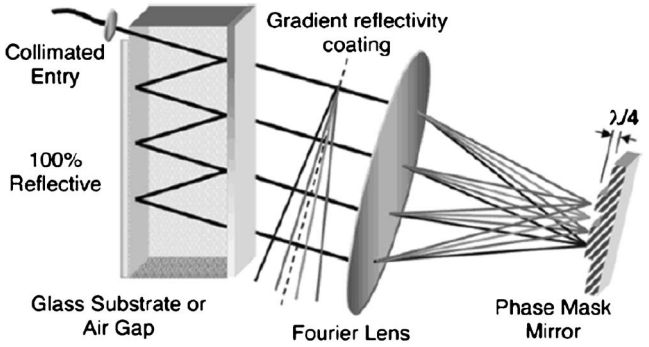

Fig. 15. VIPA setup.

FBG. The all-fiber spectral E/D based on FBG consists of a pair of step-chirped FBGs, i.e., gratings composed of spatially adjacent subgratings each of constant but constantly incremented spatial period, arranged in series and is based on the concept of spectral dispersion in time domain as opposed to the spatial Fourier domain [87]. When an input pulse is incident on the first chirped grating, the wavelengths are dispersed in time and the reflected pulse is temporally expanded. When this expanded bit is reflected from a second FBG having an opposite dispersion slope, the wavelength components are resynchronized and the original pulse is reconstituted. However, if the second grating contains phase shifts along its length these phase shifts are transferred to the reflected signal and the output pulse represents a spectral phase encoded bit. The decoder is identical to the encoder, but with the gratings connected in reverse. In the experiment reported in [87] each grating consists of eight subgratings (a spectral code with length 8). Each subgrating is of length 2.4 nm and has a reflectivity of 60% and their Bragg wavelengths increase in 0.5 nm steps from 1540.5 nm.

AWG. A promising approach to the spectral phase E/D that provides high spectral resolution along with the possibility of monolithic integration, is based on AWGs [88–90]. The operation of these methods is similar to the 4F system described in the above, i.e., a grating first spatially decomposes spectral content of the incoming light pulse, and after inserting appropriate phase shifts by a phase mask, a second grating (or in the case of a reflection type, the first grating itself) reassembles the original decomposed spectral content. In an experiment presented by Tsuda *et al.* [88] a reflection-type AWG with a diffraction order of 72 and an array of 286 waveguides was used. The resulting resolution was 12.6 GHz. A pseudorandom sequence with a length of 255 was used in the fabrication of the spatial phase filter by electron beam lithography. This was a single-user experiment in which a mode-locked laser with a pulse width of 810 fs was used. In a recent and crucial experiment an AWG-based E/D with an electro-optic phase shifter array, and which is totally monolithically integrated was constructed and reported by a research team at the University of California (UC) at Davis [89,90]. The number of AWG channels in this experiment is relatively low (eight channels), but there seems to be no severe restrictions to move to more channels. The fast response of electro-optic phase shifter (more than 10 GHz) is an important feature of this approach. None of the other reported methods could dynamically change the spectral phase mask with this ease and speed.

Finally, recently another method using reconfigurable integrated ring resonator circuits was introduced by Agrawal *et al.* [91]. In this approach the ultrashort light pulse is passed through a filter bank based on microring resonators and after appropriate phase shifts by thermo-optic phase heaters, the outputs of different branches are combined together. The code length reported here was 8. This technique also provides an integrated E/D, but the phase shift speed cannot be larger than a few kilohertz.

4.B. Coherent Time-Addressing OCDMA

This technique is essentially the direct sequence CDMA (DS-CDMA) used in radio wireless communications. For each data bit to be transmitted, a pulse train in which the polarity of pulses is determined by a pseudorandom/pseudonoise (PN) sequence (e.g., M sequence or Gold codes) is transmitted [92–94]. The desired receiver uses a simple match filter to recover the data bits. Other users who use different PN codes only produce a low intensity noise at the match-filter output.

4.B.1. Enabling Technologies

Planar lightwave circuit (PLC) technology was used in [92] to implement the E/D by monolithically integrating the required tunable delay lines, phase shifters, and combiners onto a single substrate. However because of the limitations on the code length in this technique, it seems to become obsolete. A more efficient approach using superstructure FBGs (SSFBG)—that is, an FBG with a slowly varying refractive index modulation profile imposed along its length—was adopted by Teh *et al.* [93]. When an ultrashort pulse is reflected from an SSFBG, it is transformed into a pulse with a temporal shape given by the convolution between the input pulse and the impulse response of the grating. The impulse response of a grating has a temporal profile given by the complex form of the refractive index superstructure modulation profile of the grating. If phase shifts are inserted between different segments of the SSFBG, an incident ultrashort optical pulse onto the SSFBG will generate a series of coherent short optical pulses whose phases are determined by the pattern of the phase shifts in the SSFBG. Using this technique, code lengths up to 511 could be achieved as reported by Hamanaka *et al.* [94].

4.C. Ultrashort Light Pulse Detectors

The receiver of each user in an ultrashort light pulse OCDMA system requires a thresholding device that is able to distinguish between the properly decoded pulses (uncoded pulses) and the MAI noise. The MAI signal consists of the summation of multiple improperly decoded pulses (coded pulses). Uncoded pulses have high peak power and short time duration. But, on the other hand coded pulses have low peak power and long duration. Figure 16 shows the block diagram of a typical spectrally encoded OCDMA network with M users, in which, specifically, different structures of nonlinear receivers can be used for detection purposes. In this section we intend to introduce these structures that are considered frequently in the literature as nonlinear thresholders. At the receiver, the output signal of the decoder corresponding to the ith user can be expressed as follows:

$$r_i(t) = \sqrt{G}E_{ii}(t) + \sqrt{G}\sum_{j=1,j\neq i}^{M} E_{ij}(t) + Q(t). \tag{11}$$

In the above equation G, the gain, is the total amplification and losses along the transmission line. $Q(t)$ is the amplification noise present at the receiver. $E_i(t)$ is the coded signal corresponding to the encoder of the ith user, $E_{ii}(t)$ is the properly decoded pulse at the decoder of the ith user, and $\Sigma_{j=1,j\neq i}^{M} E_{ij}(t)$ is the improperly decoded signal (MAI noise) due to all other users in the network.

Results of [13] indicate that if random codes are used at the EID, MAI noise can be modeled as a Gaussian random process. It is well-known that the amplifier noise in Eq. (11) can also be represented with a Gaussian random process. Therefore, the optimum receiver for the detection of properly decoded pulse, corrupted with MAI and amplifier noise, is a filter matched to the original uncoded light pulse. But because of the limited speed of ordinary photodiodes, implementation of the match filter is not practical. In fact, coded and uncoded pulses have equal energy in one bit duration. Therefore, an ordinary photodiode, with bandwidth limited to the bit rate, cannot distinguish between the properly decoded pulse and the MAI signal.

As shown in Fig. 16, a nonlinear optical thresholder is needed to distinguish between the coded and properly decoded signals. When the input to the thresholder is the MAI signal, with low peak power, the output should be negligible compared to the output for the properly decoded pulse. Some research groups proposed the time gating method to reduce MAI noise; see, e.g., Etemad *et al.* [86] and Wada *et al.* [95]. This

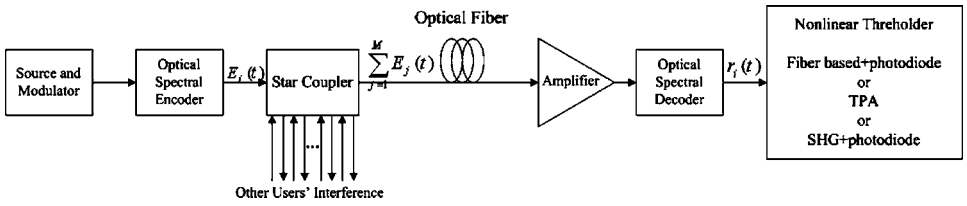

Fig. 16. Block diagram of a typical spectrally encoded OCDMA network that uses different types of thresholders for detection.

method requires a control pulse at the receiver that needs to be synchronized to the properly decoded short pulse to select the main lobe of that pulse and to reject the out of main lobe's interferences. Therefore, a fine level of timing coordination is required at the receiver. But as is known, asynchronous operation is one of the desired features of the OCDMA technique that is sacrificed in this method for the sake of interference reduction. To overcome this issue other types of asynchronous thresholders are introduced. Some other research groups proposed the use of a slot-level synchronous CDMA technique for interference and beat noise reduction [96,97]. In this method the bit duration is divided into a few time slots. The users are classified into some groups and each time slot is dedicated to a group. The users in one group transmit their signals into that time slot that is assigned to them. After encoding, the short light pulse of each user spreads in time in its dedicated time slot and does not overlap with the other group users' signals. At the receiver end of each user first the corresponding time slot should be gated with some time gating methods [96]. Therefore, similar to the chip-level time gating scheme this method also requires precise timing coordination between the users which sacrifices asynchronous operation of OCDMA systems. After slot level time gating Scott *et al.* [96] used a HNLF thresholder, which is discussed later in this paper, for interference reduction within that time slot. In this reference an OCDMA system with eight users is demonstrated. In that demonstration the bit duration is divided into two time slots and each time slot accommodates four users' signals only.

However there are a few different asynchronous methods for detection purposes. To the best of our knowledge three major types of asynchronous thresholders have been addressed in the literature up to now. These methods do not require control signal among the users and perform their detection scheme in a completely asynchronous manner.

4.C.1. Enabling Technologies for Detection of Ultrashort Pulses

Fiber-based thresholders. This type of thresholder works based on nonlinear properties of fibers when a high intensity short pulse propagates within the fiber. When an uncoded pulse or a properly decoded pulse with a high peak power propagates along the fiber, due to self-phase modulation (SPM) and other nonlinear effects such as Raman effects, an intensity dependent phase is generated and accumulated to the phase of the main pulse. This effect causes frequency spectrum broadening with the propagation of uncoded ultrashort pulses. But, if low intensity MAI propagates along the fiber, the frequency spectrum does not broaden.

Within the conventional model of SPM, the nonlinear properties of the medium are governed by the nonlinear Schrödinger equation as follows [98]:

$$j\frac{\partial A}{\partial z} = -j\frac{\alpha}{2}A + \beta_2\frac{\partial^2 A}{\partial T^2} - \gamma|A|^2 A. \tag{12}$$

In the above equation, $A(z,t)$ is the slowly varying envelope amplitude and, α, β_2, and γ represent the loss coefficient, the group-velocity dispersion (GVD) coefficient, and the nonlinear coefficient of the fiber, respectively. Considering only nonlinear effects of fiber and ignoring the loss and the dispersion, there is a closed form solution for the above equation as follows [98]:

$$A(L,t) = A(0,t)\exp[j\gamma L|A(0,t)|^2]. \tag{13}$$

A bandpass filter (BPF), having its transmission band out of the signal frequency band, allows the passing of the new frequency components generated by the SPM effect and rejects the original signal frequency components. Finally, a photodiode with a bandwidth limited to the incoming bit rate gathers the energy in one bit duration. This energy corresponds to the output of the BPF in one bit duration. It has a relatively large value for an uncoded or properly decoded pulse when compared to noise such as coded pulse propagating inside the fiber. The expressed effect is one of the simplest forms of fiber nonlinearities in which the dispersion effect of fiber is not considered. Considering dispersion, Eq. (13) does not apply exactly, however, as before, the spectrum broadening of the propagated pulse occurs if a high peak power pulse propagates along the fiber, and a BPF following the nonlinear fiber works as a nonlinear thresholder.

This technique has been applied in different forms by different research groups,

such as dispersion shifted fiber (DSF) [99], HNLF [100], holey fiber (HF) [101], and supercontinuum (SC) generation in dispersion flattened fiber (DFF) [94,102]. All the above fibers use SPM induced spectral broadening followed by a BPF. The ability of a thresholder to distinguish between coded and uncoded pulses is stated with "contrast ratio," which is defined as the ratio between the responses of the thresholder to the uncoded and coded pulses. The criterion for comparing different methods of thresholding is based on the required power to meet a predefined and fixed contrast ratio.

In [99], a group of researchers at Purdue University led by Weiner demonstrated a single-user OCDMA testbed. They have used femtosecond pulses with the duration of 275 fs and 30 MHz repetition rate. At the receiver they have used a DSF in two regimes as a thresholder. At first, a 500 m DSF with zero dispersion wavelengths equal to the central wavelength of ultrashort pulse (1559 nm) is used. A long wavelength pass filter with cutoff wavelength equal to 1569 nm is used. With these physical characteristics a contrast ratio equal to 30 dB with an average pulse power equal to 440 μW is obtained. On the other regime of DSF, a 340 m DSF with zero dispersion wavelengths equal to 1547 nm is used. In this regime the optical spectrum of the pulses lie entirely in the anomalous dispersion regime of the fiber. In this case other nonlinear effects of the fiber such as Raman effect and the resulting soliton self-frequency shift are used to distinguish between coded and uncoded pulses. A long wavelength pass filter with cutoff wavelength equal to 1577 nm is used after DSF. With this type of DSF a contrast ratio equal to 36 dB using 1.84 mW average power could be obtained.

In [100], a group of researchers at UC–Davis led by Heritage have demonstrated a four-user OCDMA testbed. They have used a 2.5 ps mode-locked pulse with 10 Gbits/s repetition rate at 1550 nm central wavelength that is generated by a fiber mode-locked laser and then compressed to a 0.5 ps mode-locked pulse source with the same repetition rate using a nonlinear fiber-based compressor they have also used for a 500 m HNLF. The specification of HNLF includes a zero dispersion wavelength equal to 1543 nm, 0.19 ps nm km dispersion at 1550 nm, dispersion slope of 0.026 ps nm^2 km at 1550 nm, effective area of 10 μm^2, and a nonlinear coefficient equal to 20 (W km)$^{-1}$. A long wavelength pass filter with cutoff frequency equal to 1568 nm is used and a contrast ratio equal to 23 dB using 25 mW average power could be obtained.

In [101], a research group led by Richardson has demonstrated a single-user OCDMA system. The pulse width and repetition rate of mode-locked pulse were 3.2 ps and 1.25 GHz for each user, respectively. They have used a 8.7 m silica holey fiber, which is a DSF fiber with the core area approximately equal to 2 μm and an outer diameter equal to 125 μm. There are many holes around the core and this causes high nonlinearity per length of the fiber, which yields short length HNLF. With this type of thresholder they could make a very short, in length, fiber-based thresholder with a nonlinearity coefficient equal to 31(W km)$^{-1}$. The contrast ratio obtained in this method is not mentioned in [98]. But following the discussions in [96], on the results of [98], the average power required for this method is stated to be equal to 2 W.

A research group at Osaka University led by Kitayama [94] has demonstrated a ten-user OCDMA system. The pulse width and the repetition rate of each user using a mode-locked laser were 1.8 ps and 1.25 Gbits/s. They have used a 2 km DFF and a 5 nm optical BPF. The central wavelength of the BPF was assumed to be around 5 nm apart from the central wavelength of the pulses (1550 nm). The zero dispersion wavelengths of the fiber are 1523.1 and 1575.2 nm. Also in [102] a contrast ratio equal to 13 dB with an operation power of less than 2 mW could be obtained by a DSF thresholder with a length of 2.5 km.

Some fiber-based thresholders were implemented with a nonlinear optical loop mirror (NOLM) [103]. The power transfer function of this nonlinear device does not have a steep threshold characteristic [102]. Therefore, its thresholding performance is not better than fiber-based thresholders, as were mentioned above. Also recently, performance analysis of a spectrally encoded OCDMA system, using fiber with SPM effect as a thresholder device, was addressed in [104,105].

TPA. In photodetectors using the TPA process, the bandgap frequency of the photodetector is chosen to be between the values of once and twice the frequency of the transmitted light [106]. Thus an electron–hole pair will be liberated from a photodetector if two photons are incident on the photodetector simultaneously [107]. In a TPA

detector the rate of photoelectrons generated in a photodetector (dN/dt) is proportional to the square of the intensity of the optical signal. Hence, we have [107]

$$\frac{dN}{dt} = \frac{\alpha}{h\nu} I(t) + \frac{\gamma}{2h\nu} I^2(t). \tag{14}$$

In the above equation $I(t)$ is the intensity of incident wave, α and γ are physical constants, h is the Planck's constant and ν is the frequency of incident wave. It can be shown that the average photocurrent output of a TPA receiver, corresponding to a Gaussian intensity input pulse

$$I(t) = I_{ave} \sqrt{\frac{2}{\pi}} \frac{T}{\tau} \exp\left(-\frac{2t^2}{\tau^2}\right)$$

can be written as follows [108]:

$$i_{ave} = \frac{e\Omega}{T} \int_{-T/2}^{T/2} \frac{dN}{dt} dt = e\Omega \left(\frac{\alpha}{h\nu} I_{ave} + \frac{\beta T}{2\sqrt{\pi} h\nu\tau} I_{ave}^2 \right). \tag{15}$$

In the above equation, τ is the input pulse width and $1/T$ is proportional to the speed of the receiver.

Since properly decoded and improperly decoded pulses have different pulse widths, a TPA photodetector can be used as a thresholder in the receiver. Some research groups, such as that at Purdue University proposed this device as a thresholder for spectrally encoded ultrashort light pulse OCDMA systems [109]. In a TPA-based thresholder if we use purely random codes with fixed average power the contrast ratio is proportional to $1/N$ in which N is the code length [109]. In reference [109] a GaAs/AlGaAs ridge p-i-n waveguide detector was used as a TPA photodetector. Also by using M sequences as the signature sequences with length 63 and with an average power of 4.7 mW one could obtain a contrast ratio approximately equal to 12 dB. One of the major advantages of TPA-based thresholders is their compactness. This feature also causes these devices to have a lower latency in response to input signal compare to fiber-based thresholders whose length is hundreds of meters and that have large response time.

Recently, the statitistical characterization of TPA photodetector in a lightwave system with optical amplifier was addressed by Jamshidi and Salehi [110]. Also the performance analysis of an spectrally encoded OCDMA system based on the proposed statistical characterization of TPA photodetector was investigated in [111] by the same authors. In [111] the performance of the system shown in Fig. 16 is compared for the two cases of SPA (single-photon absorption) and TPA photodetection. The SPA photodetector is assumed to be a conventional photodiode with a quantum efficiency denoted by η. Therefore, the photoelectrons collected in one bit duration, which is the decision variable, can be evaluated as follows:

$$Y_{i,\mathrm{SPA}} = \frac{\eta}{2} \int_0^T |C(t) + D(t)|^2 dt. \tag{16}$$

In the above equation, T is assumed to be the integration time of the SPA photodetector. $C(t)$ and $D(t)$ are the base-band representation of $\sqrt{G}E_{ii}(t)$, properly decoded signal, and $B(t) = \sqrt{G}\Sigma_{j=1,j\neq i}^{M} E_{ij}(t) + Q(t)$, MAI, and amplifier noise, which can be modeled with a Gaussian random process. Using Eq. (14), an equation similar to SPA can be evaluated for an ideal TPA photodetector, i.e., $\alpha = 0$, as follows:

$$Y_{i,\mathrm{TPA}} = k_2 \int_0^T |C(t) + D(t)|^4 dt. \tag{17}$$

In the above equation, k_2 is a constant equal to $3Vh\nu\gamma/16S^2$ [107] where V is the volume of the detector and S is the area of the TPA photodetector. h, ν, and γ are physical constants that are defined as in Eq. (14). Using the same approach as in reference [110] in obtaining the statistical model of TPA photodetector, the mean and variance of the decision variable (the number of photoelectrons) can be evaluated. Using Gaussian approximation for the distribution of the decision variable and select-

ing an optimum threshold, the error probability for both SPA and TPA receivers given l interfering users for the desired user can be expressed as follows:

$$\mathrm{BER}(l) = \frac{1}{2}Q\left(\frac{E(Y_{1,l}) - Th}{Var(Y_{1,l})}\right) + \frac{1}{2}Q\left(\frac{Th - E(Y_{0,l})}{Var(Y_{0,l})}\right). \tag{18}$$

In the above equation, $Y_{1,l}$ is the received signal when the transmitted bit is equal to 1 and there are l interfering users, and $Y_{0,l}$ is the received signal when the transmited bit is equal to 0 and there are l interfering users. Th is the threshold value for the decision variable and it is optimized to minimize the overall BER. The overall BER can be computed with averaging BER(l) over l, number of interfering users, with a binomial distribution.

Figure 17 shows the error probability of SPA and TPA receivers with different photodetector speeds using the parameters specified in Table 3. As it is observed in this figure, the performance of SPA receiver is superior to TPA receiver (with respect to error probability) when an ideal optical gating device with integration time that can be as low as the chip time (ideal case) is used. This, in turn requires the use of sophisticated time gating, which increases the complexity and the cost of femtosecond- or picosecond-based OCDMA receivers. However as the integration time increases, i.e., using lower speed photodetectors, the performance of TPA receivers surpasses that of SPA. As is shown in Fig. 17, the performance of the TPA receiver is far superior to that of the SPA receiver when a typical photodetector with a speed of 25 GHz is used. From Eq. (15) the first term is due to the effect of SPA (the linear region) and the second term (the nonlinear region) is due to the TPA effect. Therefore, the photocurrent due to TPA effect is inversely proportional to the speed of the receiver and also inversely proportional to the input pulse width. As is observed in Table 3, the pulse width is constant and the speed of the receiver varies. For this paper we have considered three different speeds. If the speed of the receiver is 250 GHz and 2.5 THz, the SPA term will be strictly dominated until the speed of the receiver gets as small as 25 GHz when TPA becomes the dominant term with increasing average power.

SHG. When an optical wave of frequency ω_0 propagates in a dielectric material a second-harmonic wave of frequency $2\omega_0$ is generated and traversed to the end of the material. This phenomenon occurrs efficiently, if the phase velocity of the fundamental and the second-harmonic waves are matched. As we know, coded and uncoded pulses have broad frequency spectrum and it is not possible to satisfy the phase-matching condition for all sum frequency components. In [112] propagation of broadband pulses in a dielectric material considering SHG is addressed. When a broadband pulse with frequency spectrum $A_1(\omega)$ propagates in the SHG dielectric material (assuming phase-matching conditions are satisfied), a second-harmonic wave with frequency spectrum $A_2(\omega)$ is generated as follows [113]:

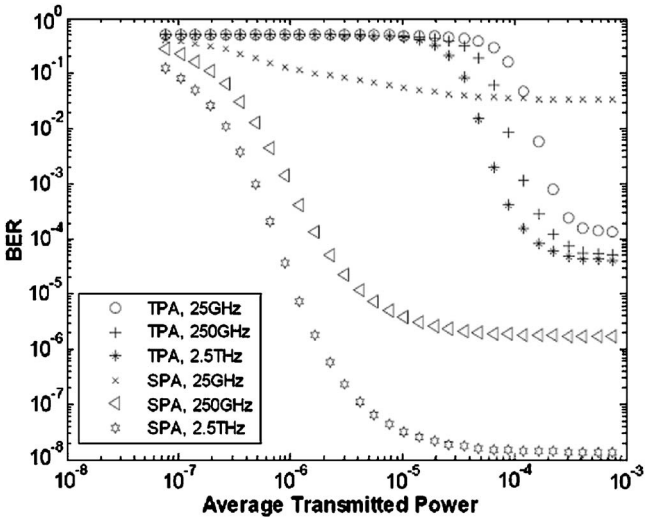

Fig. 17. BER versus average transmitted power for asynchronous transmitters using TPA and SPA receivers with different photodetector speeds.

Table 3. Typical Parameters Used in Ref. [108]

n_{sp}	Spontaneous emission factor	1.1
T_r	Receiver temperature	300 °K
R_L	Load resistance	1000 Ω
T_c	Width of ultrashort pulse	400 fs
η	Quantum efficiency	0.9
N_0	Code length	250
M	Number of users	20
R	Bit rate	1 Gbit/s
G_{amp}	Gain of amplifier	1000 (30 dB)
L_1	Total path loss before amplification	8 dB
L_2	Total path loss after amplification	5 dB

$$A_2(\omega) = \left[2\int_0^{\infty} A_1(\omega/2 - \omega')A_1(\omega/2 + \omega')\mathrm{d}\omega' \right] D(\omega). \tag{19}$$

In the above equation ω and ω' are the frequency detuning from $2\omega_0$ and ω_0, respectively (ω_0 is the carrier frequency of the fundamental wave and $2\omega_0$ is the carrier frequency of second-harmonic pulse). $D(\omega)$ is the transfer function of a low-pass filter, which represents the effect of the phase-matching condition and is expressed as follows [113]:

$$D(\omega) = \Gamma L \sin c(\omega\alpha L/2). \tag{20}$$

In the above equation L and Γ are the length and nonlinear coupling coefficient of dielectric material, respectively, and $\alpha = 1/v_{g_1} - 1/v_{g_2}$ is produced from the group-velocity mismatch (GVM) between the fundamental pulse, with group velocity v_{g_1}, and the second-harmonic pulse with group velocity v_{g_2}.

Based on the relative value of the length of SHG material (crystal), two extreme cases could be considered, namely, thin crystal and thick crystal.

Thin crystal case. In this case, which occurrs when the length of the crystal is short, the energy in the second harmonic pulse (E_{SHG}) can be represented as follows [113]:

$$E_{\text{SHG}} \propto \int_{-\infty}^{+\infty} \left| \int_{-\infty}^{+\infty} A_1(\omega/2 + \omega')A_1(\omega/2 - \omega')\mathrm{d}\omega' \right|^2 \mathrm{d}\omega = \int_{-\infty}^{+\infty} I_1^2(t)\mathrm{d}t. \tag{21}$$

Thick crystal case. In this case, which occurrs when the length of the crystal is long, the energy in the second-harmonic pulse (E_{SHG}) can be evaluated as follows [113]:

$$E_{\text{SHG}} \propto \left| \int_{-\infty}^{+\infty} A_1(\omega')A_1(-\omega')\mathrm{d}\omega' \right|^2. \tag{22}$$

An ordinary photodiode sensitive to the wavelength equal to the half of the fundamental wavelength, gathers the second-harmonic energy and is evaluated in Eqs. (21) and (22).

In [114], the research group at Purdue University used a periodically poled lithium niobate (PPLN) crystal in thick regime as a thresholder. They used a commercial PPLN crystal 20 mm long and 0.5 mm thick. A different coding–decoding scheme is represented because of the correlation form of Eq. (22). The orthogonal Walsh–Hadamard codes with lengths of eight, which are often used in synchronous OCDMA, are considered as signature sequences of the users. In this encoding–decoding scheme, the spectrum of short pulse is split in half, the transmitter uses the lower half of the spectrum and encodes it with its corresponding phase code (C_1). The receiver uses the upper half of the spectrum and encodes it with its corresponding phase code (C_2). If C_1 and C_2 are matched (C_2 is complex conjugate of C_1), the second-harmonic energy in Eq. (22), will have a high value and otherwise it has a low value (ideally equal to zero). They have investigated only the performance of PPLN crystal as a correlator element in spectral domain. Therefore, in their system one code is used as the desired user's code and another code from the Walsh–Hadamard family is used as the interference, and the operation of this system for interference suppression with a large

number of interfering users was not considered.

Also in [97], a thick PPLN crystal with a length equal to 67 mm has been used by the same group at Purdue University with the conventional encoding–decoding scheme in which the spectrum is encoded entirely with *M* sequences. In this reference the authors demonstrate a four-user spectrally encoded OCDMA system in which the users are slot-level synchronous. The pulse width and repetition rate of the mode-locked laser that is used in their system are 400 fs and 2.5 Gbits/s and the central wavelength of the mode-locked pulse is near 1542 nm. In this experiment they claim that they could obtain full interference suppression using PPLN crystal in which only 200 fJ/bit energy is required. This level of required power is as much as 2 orders of magnitude lower than fiber-based thresholders.

Among all the detection schemes discussed in the previous section the SHG method in PPLN crystals requires very low power compare to other methods [102,113,114]. But this method is polarization dependent, which causes an additional polarization mode partition noise [102]. In fact, in asynchronous OCDMA systems beat noise is an important noise term, which is very sensitive to polarization states of signals [102]. The TPA method is featured by its compactness but requires high power compare to SHG. On the other hand, fiber-based thresholders have less polarization dependency and even though they require high power compared to SHG, they are widely used by many research groups.

5. Applications of OCDMA in Data Networks

Up until this section we have discussed many research activities and the results of various OCDMA techniques and their corresponding performance in physical layer. However, employing OCDMA in data communication networks has gained a lot of momentum recently, and in general can be categorized into three major classes. The first category is the design and the performance analysis of code-based optical routers and switches in all-optical switching networks [115–122]. In addition to the core routing networks, many researchers have demonstrated and studied the performance and effectiveness of the OCDMA applications in local area and access networks, which constitute the second category [123–138]. And finally the third category consists of some emerging research to devise, analyze, and study the feasibility of employing OCDMA to set up wireless optical networks for both indoor and free-space environments [139–148].

5.A. OCDMA-Based Switching in Core Networks

The increasing demand on communication bandwidth and capacity makes the optical networks the major candidates and an inevitable choice for the core of large scale networks. While growing optical technologies makes data transmission fast enough, limited speed of switching and routing modules along the traffic flow path due to the limited speed of electronic processing become the limiting factor [115,116]. Hence, there is a great tendency towards all-optical routing and switching in order to overcome the shortcomings of optical–electrical–optical conversions.

As we discussed in previous sections, recent implementations of several multigigabits per second OCDMA systems [117] show the capabilities of such techniques in several gigabits per second data communication systems. Furthermore, requirements for future all-optical networks and the potential of OCDMA in satisfying them, such as all-optical processing, simplified and decentralized network management, inherent consistency with traffic bursts, improved spectral efficiency, and enhanced security have attracted increased attention to this advanced and fundamental multiple-access technique.

Kitayama and Murata [116] have proposed a high-speed photonic access node employing code-based photonic add–drop multiplexing (PADM) for packet networks. Despite other traditional optical add–drop multiplexers (OADMs), such as wavelength OADMs, PADM handles traffic flow of a single wavelength on a packet by packet basis, which means it drops the arriving packets, adds the generated packets in the node to the flow, and bypasses the node when required [116]. They have also proposed two applications for PADM in optical networks, studied the proposed applications, and concluded that PADM can effectively be used in the all-optical networks (especially optical thresholding devices and switches). They have showed that their schemes have

acceptable performance and predicted its packet processing capability to be as high as 200 gigapackets per second [116]. Wada and Kitayama [117] have addressed a 10 Gbit/s experimental demonstration of photonic IP routing in which IP addresses are mapped onto optical codes and the photonic router takes the optical correlation between an incoming optical code and those in the address bank. The experimental results show that packets consisting of eight-chip long header and 64-bit long burst payload data can be generated and optically routed along the optical domain [117].

In addition to bandwidth demand, quality of service and traffic engineering are the other critical issues in the future core networks, which have made multiprotocol label switching (MPLS) to be the dominant trend in IP-based networks. One of the evolutionary scenarios of future photonic backbone networks is generalized MPLS (GMPLS). GMPLS is characterized by using a set of values of wavelengths as labels. However while employing wavelengths as labels in GMPLS networks is useful it has some major shortcomings, such as coarse data granularity, which implies that the transmitted data by one label consumes the entire wavelength capacity. To address this shortcoming of wavelength-based GMPLS, Kitayama and Murata have presented an optical code(OC)-based MPLS protocol [118]. They take the OC as a label identifier attached to the data and the detection is carried on by performing optical correlation between the incoming label code and the OC-label entries. They have investigated a packet switch architecture to perform switching tasks as well as increasing the bandwidth efficiency. OC-MPLS have finer data granularity and it can be enabled on burst packet switching to utilize link capacity. They have also presented an OC-labeled photonic packet switch architecture incorporating WDM buffering and scheduling, and optical implementation of longest prefix match for the presented switch [118].

To build a working label switched backbone, it is required to implement label swapping and translation capability on the switches; this topic is considered by Jiang *et al.* [119] by means of simulation and experiment. They have shown dynamic and programmable all-optical code translation as an efficient way to increase user counts and/or reduce the number of required codes in a spectrally phase coded OCDMA testbed. One and two-stage code translation is analyzed and simulated and it is shown that each translation induces a less than 0.9 dB power penalty. Moreover, due to pulse degradation caused by code translation and multistage code translation, emulation on a loop pulse shaper is considered in the article. The authors concluded that using OCDMA E/Ds as code translator and employing their presented code translation function, provide all-optical multistage code swapping in a simple, linear, and low delay fashion to become a promising scheme in future optical switching networks [119].

A scheme for full E/Ds has been presented in [120] that generates and processes a set of N optical codes simultaneously and can be used in GMPLS networks. Furthermore, to be used at the ingress node of a GMPLS enabled network, Cincotti demonstrated the idea of using standard multiplexers such as Mach–Zehnder interferometer (MZI) or waveguide gratings to generate OCs [121]. The paper demonstrates that the OCs can be generated by a device called a generalized MZI, which consists of two multimode interfering (MMI) couplers, an array of N waveguides, and N optical phase shifters. It then computes the performance of the proposed E/Ds analytically to conclude that standard multiplexers can be designed as full E/Ds for 1-D and multidimensional optical codes [121].

A group of researchers led by Salehi at the Optical Networks Research Laboratory at Sharif University of Technology have addressed the feasibility and advantages of a novel GMPLS-based switch fabric that consists of passive OCDMA E/ds, optical hardlimiters (OHL), optical cross connects (OXC), and an optical amplification block that uses spectrally phase encoded OCDMA codes as labels [122]. The proposed fabric can be based both on dynamic E/Ds and static OXC or a dynamic OXC and regular E/Ds to guarantee full connectivity. Just after the path setup phase the switch will perform all optically, with no electrical processing, at the bit level, i.e., every single bit is switched separately. This is highly desirable for bursty data traffic and delay–jitter sensitive multimedia transmissions. Furthermore, bit-level switching is required to overcome granularity issue of traditional GMPLS networks [122]. The authors describe the switch architecture and characteristics and derive its performance metrics, such as throughput, blocking probability, packet loss rate, and setup delay. Finally, the authors conclude that the packet-based photonic label switching router can gain various inherent advantages of the OCDMA technique when implemented

for multimedia and data based systems. The results show that the proposed system can conceptually have an excellent performance. Also the system can coexist with a current wavelength division multiplexed-based systems on the same infrastructure, which can prove to be important in case of gradual deployment [122].

As it is clear from the above discussion, OCDMA, and its access with its various schemes such as OOCs and spectrally encoded OCDMA, has found its way into data communication networks in different aspects. In fact there has been a general research trend towards feasibility analysis and implementational challenges of OCDMA both in fiber-optic and wireless networks.

5.B. OCDMA-Based Fiber LAN and Access Networks

There are many research groups that have addressed the design, and have examined the network or data link layer issues, and have proposed novel protocols for fiber-based networks [123–138]. Hsu and Li [123] have examined OCDMA techniques in a slotted packet network, with both time- and frequency-hopping schemes. They have considered both centralized and distributed communication networks and have derived system throughput and delay using forward error correction codes (FECs) assuming fixed sized packets and random time of arrival for the packets. They have concluded that the desired throughput can be achieved by proper selection of code length and/or number of frequency slots, which correspond to the processing gain of the system [123]. Performance analysis of an unslotted network is also presented by Hsu and Li [124], which is a more realistic and robust assumption in data communications because the number of interferers might change due to bursty nature of the received traffic at each node with no required timing coordination among the users. Performance evaluation of an unslotted network is obtained using two approximation methods; one for small packet length and the other for large packet length. With the performance of wavelength- (frequency-) hopping–time-spreading optical networks at hand, Stock and Sargent tried to compare their performance to that of a WDMA network in [125]. They showed that OCDMA systems have a higher utilization than WDMA in certain regimes of operation.

Channel coding may be used to improve the physical and data link performance, i.e., BER and throughput–delay [126,127]. Using Reed–Solomon or convolutional codes to improve physical performance is considered by Dale and Gagliardi [126] and Azmi *et al.* [149]. Kim and Poor [127] have applied turbo codes to analyze and simulate the performance of a slotted OCDMA network employing binary pulse-position modulation (BPPM) in terms of packet throughput–delay. They concluded that turbo coding can be very useful in improving the packet throughput and in increasing the number of users of an OCDMA network for a given BER requirement. Moreover, the insertion of channel E/Ds into an OCDMA network has little cost impact on the overall network implementation [127].

In 2003, Shalaby began a series of articles on the performance and the protocols of the data link layer for an OCDMA packet network using OOCs [128–131]. First, he suggested two different protocols, namely, with and without pretransmission coordination [128]. Both protocols assume that all of the available codes are in a code pool and each user is assigned a code randomly when it decides to transmit data. However, in the first protocol the code is excluded from the pool once it is assigned for a data transmission, while in the latter the codes are never removed from the pool, which gives the network the ability to support more users and gain more throughput. A variation of the second protocol is proposed to eliminate the need for pretransmission coordination in which the users are assigned a code once they become associated to the network. The paper attempts to address the steady-state system throughput and average packet delay metrics for both protocols using correlator and chip-level receivers. In [128] it is concluded that the first protocol is suitable for the correlator receiver while the second protocol improves the average throughput and delay for a network with chip-level receiver. Suggesting the above medium access protocols, Shalaby analyzed the performance of a random access protocol, called *round-robin receiver transmitter* (R^3T) for the same networks [129] in order to answer some important questions that were not addressed in [128]. Proposing the R^3T protocol and its corresponding state diagram, he evaluated the effect of multipacket messages, packet lost or error, propagation delay, and the tuning time on the performance of the data link layer using equilibrium point analysis. The results show the implementation plausibility of

OOC-based random access protocol having acceptable throughput, delay, and protocol efficiency in various situations [129]. Shalaby considered go-back n as the retransmission algorithm in [127]. However, it was shown in [130] that the link layer can attain better performance utilizing selective retransmission in the case of packet loss, but the protocol is more complicated and requires more buffer capacity in both receiver and transmitter. In the continuation of the above research in [131] an OCDMA medium access control (MAC) protocol is suggested that supports variable size window in the link layer to transmit variable length data employing error control codes. The authors have presented an accurate analysis of the proposed MAC protocol and concluded that the sliding window with variable size algorithm can enhance the system performance.

Optical access networks are considered the networks of choice in recent years [132], especially in FTTH applications (see Fig. 18), and OCDMA is fast becoming one of the main contenders for FTTH [137,133–136,138]. Pfeiffer *et al.* [133] reported an experimental setup in order to employ OCDMA in an access network with eight asynchronous users with a total capacity of 1.25 Gbits/s. They used Fabry–Perot filters at the transmitter to shape the emitted spectra and at the receiver a Mach–Zehnder filter is tuned to the same free spectral range as in the transmitter for the detection purposes. This technique allows for maximum transmission of optical power through the receiver filter. Furthermore a detailed performance analysis of the same system is presented in [134]. To satisfy the granularity need and to improve the network flexibility supporting a number of users and increasing the number of channels in metropolitan and access area Pfeiffer *et al.* [135] proposed and analyzed a network based on hybrid optical multiplexing techniques including wavelength, code, and time division multiplexing. When applied to optical packet transmission they showed that the approach enables several hundred all-optical channels between end users and the central hub with average bit rates up to 100 Mbits/s per channel while keeping the installation and maintenance cost at a minimum [135]. Furthermore, the authors suggested a special form of spectrally encoded CDM to enhance WDM networks, to guarantee independence of the optical CDM multiplexing scheme from the network architecture. Taking cross talk and intensity noise into account the authors concluded that even by using insensitive to poor component specification and drift, the network can be implemented having an appropriate performance. Schmuck *et al.*[136] presented the implementation of a bidirectional optical CDMA system within the access part of the German KomNet field trail in the Berlin area operating at 155 Mbits/s per channel in both upstream and downstream directions over a pair of 20 km single-mode fiber and having four independent optical channels in each direction. The authors demonstrated and measured an appropriate BER in the field while it enabled the transmission of, e.g., ATM packets. Kitayama *et al.* [137] have suggested a novel approach in passive optical networks (PON) to bring gigabit transmission for both the uplink and downlink using OCDMA over WDM-PON [135]. Performance analysis of

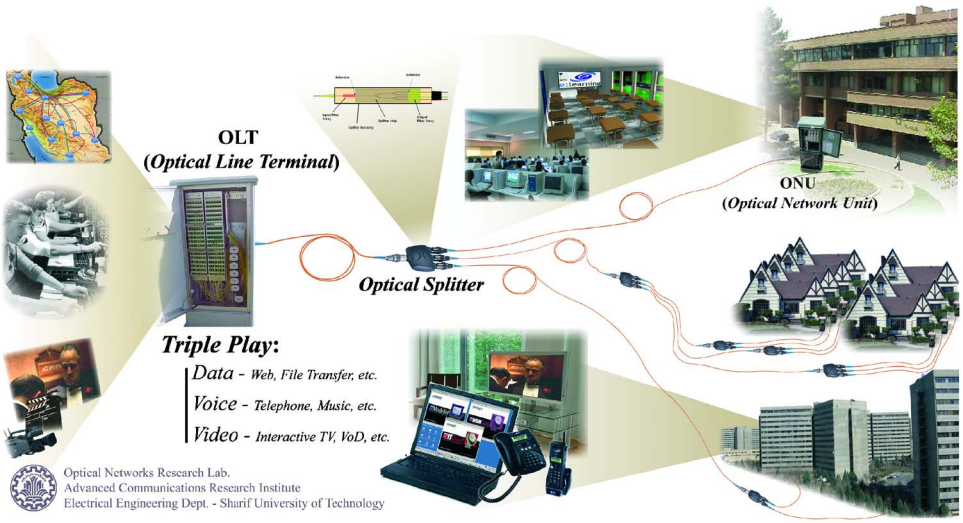

Fig. 18. FTTH architecture and services.

overlaid OCDMA channels on WDM grids to increase the system capacity is carried on in [137] in terms of BER and power penalty. Furthermore, the experimental results in [137] have shown the feasibility of a gigabit OCDMA system. Kitayama *et al.* [138] presented more discussions on OCDMA over WDM PON, and analyzed the system architecture and cross talk in the presence of WDM channels. It was shown that OCDMA over WDM PON can simultaneously provide multigigabit per second uplinks and downlinks to sufficient number of users while suppressing the WDM interchannel cross talk by taking advantage of the reflection spectrum notches of the SSFGB E/D [138].

As is clear from the above discussions, employing OCDMA in local area and access networks is fast becoming the technique of the choice for future optical networks. Therefore one can expect this trend will continue to grow through many research groups worldwide.

5.C. Wireless OCDMA

5.C.1. Indoor OCDMA Communications

Wireless optical LANS have been the subject of considerable research and implementation activities due to some of their unique features that distinguish them from traditional radio communication networks. Also it is believed that wireless optical LANs will grow in importance where security is important or where using a radio frequency band would not be economical or safe due to electromagnetic effects [139–148]. Employing OCDMA techniques has been considered in the literature to implement a diffused-channel-based indoor access network [142–148]. Elmirghani and Cryan have considered the use of a hybrid PPM–OCDMA system [142] to be implemented in an indoor infrared network. Marsh and Kahn [143] have examined the properties and compared several multiple access strategies for downlink channel sharing infrared cellular network. They assumed a hexagonal cellular scheme and a reuse factor of three, where base stations are placed at the center of each cell. Their results show that optical frequency division multiple access (FDMA) and m-sequence CDMA reuse strategies are the worst and the system implementation is plausible using TDMA and OOC enabled CDMA techniques. In fact they have concluded that for the cell radii above $3m$, CDMA using OOC sequences require approximately the same single-to-noise ratio (SNR) (i.e., transmission power) as TDMA with OOK and 2-PPM to achieve a worst case BER.

Zahedi *et al.* [144] have proposed a photon counting approach to analyze the performance of several modulation techniques using OOC as a multiple-access algorithm in the downlink channel of an indoor infrared CDMA network. The results show that the transmission can be performed well-below ambient noise power with transmission power that satisfies eye-safety power regulations. They have also suggested an M-ary modulation method using OOC in the same system [145]. This modulation technique uses the cyclic shifts of OOCs to send more information when sending one signature code [145].

Ghaffari *et al.* [146] have studied the practical digital design concepts in the implementation of a typical CDMA-based infrared network prototype (Fig. 19). They evaluate the performance of various types of receivers, namely, correlator, hard-limiter +correlator, and chip-level detector in a typical wireless OCDMA indoor LAN based on the photon counting process. Considering the implementational criteria, digital structures were introduced. The results of their paper show that correlation+hard-limiter not only obtains the best performance among other receiver structures, such as simple correlator and chip-level detection; it constitutes a simple implementational structure. However, the chip-level detection performance approaches that of correlation+hard-limiter in the high-power region. For the synchronization circuit design the performance of two algorithms for OOC-based OCDMA networks, namely, simple serial-search and multiple-shift are studied. Furthermore, they study a synchronization method based on match filtering and show that it presents a much better performance in the context of wireless OCDMA system and results in reducing the number of required training bits for the synchronization circuit operation. In this work the digital tracking circuit was evaluated by considering the effect of the sampling rate on its performance. The authors concluded that the

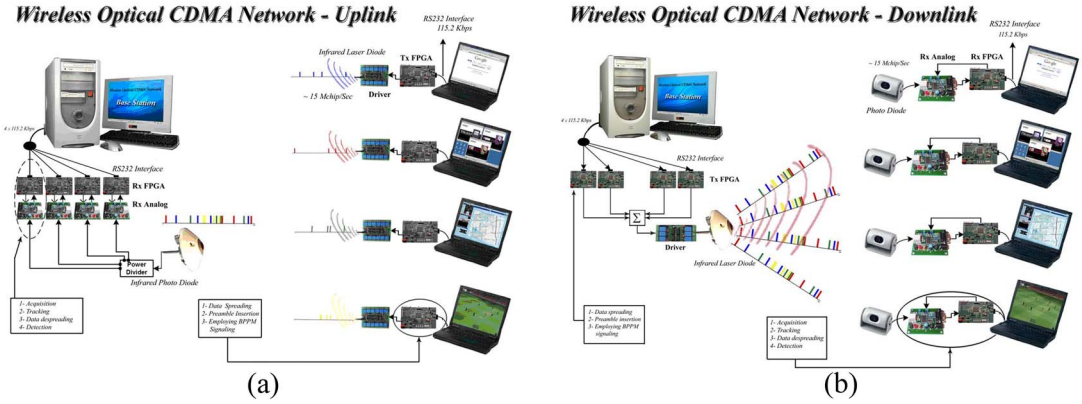

Fig. 19. Schematic of a typical wireless optical CDMA LAN (a) uplink and (b) downlink structure.

results of various stages of the proposed wireless OCDMA LAN strongly indicate the viability and the importance of such networks in certain applications.

Just like radio CDMA networks, the near–far problem has a considerable effect on a wireless OCDMA performance; therefore it is required to use power control for the uplink transmission in such networks as well. The analysis of power control and its effectiveness for the OOC infrared networks is derived by Aminzadeh-Gohari and Pakravan [147] for various cases. While enabling power control algorithm is basically important in wireless infrared CDMA networks (Fig. 19), it can be easily used for quality of service (QoS) provisioning in terms of reliability (i.e., BER), which is considered in [147]. The authors suggest an unfair power control algorithm that gives permission to high-priority users to transmit at a higher power level to achieve better error probability [148].

5.C.2. Atmospheric OCDMA Communications

Despite the complete success of optical fibers as information highways and their use in the infrastructure of the communication network, its deployment speed has been limited by some economic issues. Though it seems apparent that fibers would serve as the indispensable building block of access networks in the middle-term future, the short-term and less costly solutions using free-space optical links have received increasing attention [Fig. 20(a)].

Since in taking fiber to the home and to the desk, the major expenses are due to nontechnical operations, such as digging and installation in metropolitan areas, free-space optical link by virtue of its very simple construction leads to temporary and eas-

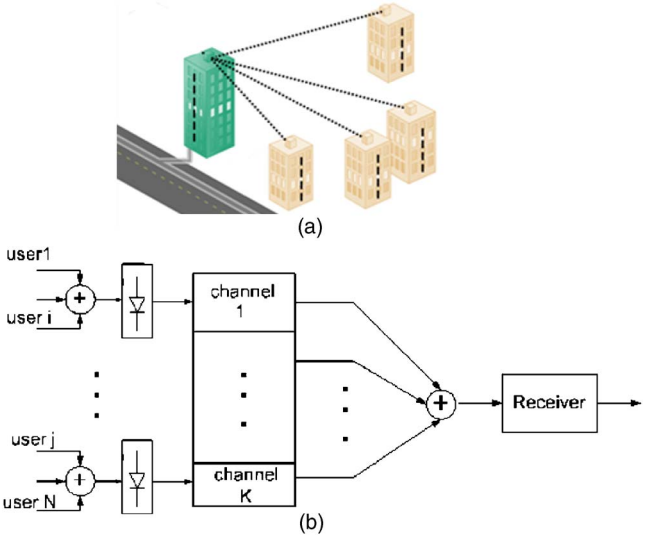

Fig. 20. Free-space optics (a) placement of transceivers on buildings. (b) CDMA compound optical channel structure.

ily reconfigurable high-speed access to the core network. Such a system also has the inherent advantages of optical domain over radio and cable solutions. It is abundant in bandwidth supply and needs no frequency licenses.

In a free-space optical channel, in addition to standard sources of noise, which are present in most optical communications, there are some particular degrading noise sources that are specific to atmospheric channel. Atmospheric loss blocks reliable data communication except in clear weather. Fortunately it has been experimentally proven that building links with a practically low probability of outage is feasible in almost all actual climatic conditions. Atmospheric links are also problematic in that they suffer from air turbulence that causes some fading (slow fading) in the received power. Such fading would be mitigated by standard communication techniques known as diversity techniques. Spatial diversity techniques have proven to be the most efficient and are realized by using multiple transmitters and/or multiple receivers.

While optical links have been widely studied and are commercially available today, sharing a physical channel between multiple users via multiple-access techniques has not been considered until recently. Ohtsuki [150] proposed application of OOC together with PPM forming an OCDMA atmospheric link. He analyzed the system using correlator receiver and concluded that for strong fading, error probability has a floor that cannot be avoided without resorting to error correction coding.

Hamzeh and Kavehrad [151] argued that synchronous OCDMA using Walsh–Hadamard codes reaches rates that are not achievable in an asynchronous system under strong fading. Jazayerifar and Salehi [152] studied a problem by considering various detection structures, namely, correlator and chip-level receivers using optical amplifiers, receiver diversity technique, and some kind of internal coding scheme [Fig. 20(b)]. In this work they took into account all sources of noise in a semi-classical photon counting approach leading to an analytically exact evaluation of performance under practical conditions. Their results indicate that such systems can be implemented using practical parameters.

6. Summary and Conclusion

In this paper I have presented a comprehensive review and discussion on incoherent and coherent OCDMA techniques, and their corresponding applications. In particular, I discussed the pros and cons of each of the above techniques, their enabling technologies, devices, and modulation schemes needed for their optimum implementations.

Depending upon a particular application and the medium in which it is to be applied, one may choose an OCDMA technique from the above two categories that suits the application and the medium in the best possible way. For example, for optical wireless and free-space applications, incoherent OCDMA techniques based on OOC codes are the most viable and robust techniques to be implemented. This is because incoherent OCDMA requires a simple intensity-modulation–direct-detection scheme that is also quite resistant to the anomalies of wireless optical channels such as phase fluctuation and optical multipath channel.

On the other hand spectrally phase encoded OCDMA can be considered as among the most advanced and promising OCDMA techniques introduced to date with throughputs that can reach as high as hundreds of gigabits per second. This technique is beginning to enjoy the benefits of some of the advanced and developed optical devices, such as erbium-doped fiber amplifiers, arrayed waveguide gratings, fiber Bragg gratings, semiconductor mode-locked lasers, all-optical thresholder, and dispersion compensation elements, in order to place itself among the most viable contenders in fiber-to-the-home (FTTH) network applications. Furthermore, spectrally phase encoded OCDMA techniques can be applied in environments where low probability of intercept and immunity from jamming are of utmost importance. However, if the available laser sources remain to be the simple and ubiquitous laser diode with high phase noise then the only viable techniques will be the incoherent 1D and 2D OCDMA.

As opposed to the common belief, this technique, which requires a much simpler encoder–decoder and detection scheme, has by no means been explored to its maximum potential. Our recent study of the use of the optical AND logic gate for the detection of OOC codes is testimony to this fact.

As discussed in this paper using the optical AND logic gate can improve the system performance drastically while simultaneously allowing one to use a more relaxed OOC structure with a much larger cardinality. Cardinality of OOCs with cross-correlation value equal to 1 was always considered to be the major weakness of incoherent 1D and 2D OCDMA systems. This bottleneck is removed by the use of advanced nonlinear optical logic gate elements such as the AND gate. It is our belief that the ultimate quest for establishing all-optical processing in incoherent OCDMA systems and data networks will highly depend upon certain key enabling technologies and devices such as binary digital optical logic gate elements. Hence the next frontier in exploring OCDMA techniques is to explore optical combinational logic functions (such as AND, NAND, XOR, OR, NOR, etc.) and devise methodologies that are applicable in optical data networks using OCDMA techniques.

The success of OCDMA will definitely rest upon maturing technologies but more importantly it depends on finding the right application where OCDMA features will stand out when compared to other multiple access techniques. We have highlighted and discussed such applications in this paper. For us wireless OCDMA LAN, free-space OCDMA systems, and FTTH are the major applications where OCDMA will surely shine and succeed for the future optical communication system.

Acknowledgments

I acknowledge the support of the Iran Hi-Tech Center and Iran National Sciences Foundation (INFS). The preparation of this paper would not have been possible if it were not for the help of my highly talented graduate students from the Optical Networks Research Laboratory (ONRL) at the Department of Electrical Engineering at Sharif University of Technology. Specifically, I extend my thanks and appreciation to the following students: B. M. Ghaffari, A. Aminzadeh-Gohari, F. Javaherian, M. Farhang, M. D. Matinfar, M. M. Alem, K. Jamshidi, S. Mashhadi, and S. Khaleghi.

References

1. J. A. Salehi, "Emerging optical code-division multiple-access communications systems," IEEE Netw. Mag. **3**, 31–39 (1989).
2. J. Ratnam, "Optical CDMA in broadband communication-scope and applications," J. Opt. Commun. **23**, 11–21 (2002).
3. B. Moslehi, J. W. Goodman, M. Tur, and H. J. Shaw, "Fiber-optic lattice signal processing," Proc. IEEE **72**, 909–930 (1984).
4. P. A. Davies and A. A. Shaar, "Asynchronous multiplexing for an optical-fiber local area network," Electron. Lett. **19**, 390–392 (1983).
5. E. Marom, "Optical delay line matched-filters," IEEE Trans. Commun. **25**, 360–364 (1978).
6. J. A. Salehi, "Code division multiple-access techniques in optical fiber networks—Part I: fundamental principles," IEEE Trans. Commun. **37**, 824–833 (1989).
7. J. A. Salehi and C. A. Brackett, "Code division multiple access techniques in optical fiber networks—Part II: system performance analysis," IEEE Trans. Commun. **37**, 834–842 (1989).
8. F. R. K. Chung, J. A. Salehi, and V. K. Wei, "Optical orthogonal codes: design, analysis, and applications," IEEE Trans. Inf. Theory **35**, 595–604 (1989).
9. J. Y. Hui, "Pattern code modulation and optical decoding—A novel code-division multiplexing technique for multifiber network," IEEE J. Sel. Areas Commun. **SAC-3**, 916–927 (1985).
10. P. R. Prucnal, M. A. Santoro, and T. R. Fan, "Spread spectrum fiber-optic local area network using optical processing," J. Lightwave Technol. **LT-4**, 547–554 (1986).
11. G. J. Foschini and G. Vannucci, "Using spread-spectrum in a high-capacity fiber-optic local network," J. Lightwave Technol. **6**, 370–379 (1988).
12. A. M. Weiner, J. P. Heritage, and J. A. Salehi, "Encoding and decoding of femtosecond pulses," Opt. Lett. **13**, 300–302 (1988).
13. J. A. Salehi, A. M. Weiner, and J. P. Heritage, "Coherent ultrashort light pulse code-division multiple access communication systems," J. Lightwave Technol. **8**, 478–491 (1990).
14. H. Chung and P. Vijay Kumar, "Optical orthogonal codes—new bounds and an optimal construction," IEEE Trans. Inf. Theory **36**, 866–873 (1990).
15. S. M. Johnson, "A new upper bound for error-correcting codes," IRE Trans. Inf. Theory **IT-8**, 203–207 (1962).
16. N. Miyamoto, H. Mizuno, and S. Shinohara, "Optical orthogonal codes obtained from conics on finite projective planes," Finite Fields and Their Applications **10**, 405–411 (2004).
17. C. S. Weng and J. Wu, "Optical orthogonal codes with nonideal cross-correlation," J. Lightwave Technol. **19**, 1856–1863 (2001).
18. G. C. Yang and T. E. Fuja, "Optical orthogonal codes with unequal auto- and cross-correlation constraints," IEEE Trans. Inf. Theory **41**, 96–106 (2001).

19. G. C. Yang, "Some new families of optical orthogonal codes for code-division multiple-access fiber-optic networks," IEE Proc.-Commun. **142**, 363–368 (1995).
20. W. Chu and C. J. Colbourn, "Optimal $(n,4,2)$-OOC of small orders," Discrete Math. **279**, 163–172 (2004).
21. H. Charmchi and J. A. Salehi, "Outer-product matrix representation of optical orthogonal codes," IEEE Trans. Commun. **54**, 983–989 (2006).
22. M. Azizoglo, J. A. Salehi, and Y. Li, "Optical CDMA via temporal codes," IEEE Trans. Commun. **40**, 1162–1170 (1992).
23. S. Mashhadi and J. A. Salehi, "Code division multiple-access techniques in optical fiber networks—Part III: optical AND gate receiver structure with generalized optical orthogonal codes," IEEE Trans. Commun. **45**, 1457–1468 (2006).
24. S. Bitan and T. Etzion, "Constructions for optimal constant weight cyclically permutable codes and difference families," IEEE Trans. Inf. Theory **41**, 77–87 (1995).
25. R. Fuji-Hara and Y. Miao, "Optical orthogonal codes: their bounds and new optimal constructions," IEEE Trans. Inf. Theory **46**, 2396–2406 (2000).
26. W. Chu and S. W. Golomb, "A new recursive construction for optical orthogonal codes," IEEE Trans. Inf. Theory **49**, 3072–3076 (2003).
27. C. Ding and C. Xing, "Several classes of $(2^m-1,w,2)$ optical orthogonal codes," Discrete Appl. Math. **128**, 103–120 (2003).
28. C. Ding and C. Xing, "Cyclotomic optical orthogonal codes of composite lengths," IEEE Trans. Inf. Theory **52**, 263–268 (2004).
29. M. M. Alem, "Analysis and design of optical orthogonal codes using matrix algebra," M.Sc. thesis (Sharif University of Technology, 2006).
30. H. M. Kwon, "Optical orthogonal code division multiple access system—Part I: with avalanche photodiode noise and thermal noise," IEEE Trans. Commun. **42**, 2470–2479 (1994).
31. T. Ohtsuki, K. Sato, I. Sasase, and S. Mori, "Direct-detection optical synchronous CDMA systems with double optical hard-limiters using modified prime sequence codes," IEEE J. Sel. Areas Commun. **14**, 1879–1887 (1996).
32. T. Ohtsuki, "Performance analysis of direct-detection optical asynchronous CDMA systems with double optical hard-limiters," J. Lightwave Technol. **15**, 452–457 (1997).
33. H. M. Shalaby, "Chip level detection in optical code division multiple access," J. Lightwave Technol. **16**, 1077–1087 (1998).
34. L. B. Nelson and H. V. Poor, "Performance of multiuser detection for optical CDMA—Part I: error probabilities," IEEE Trans. Commun. **43**, 2803–2811 (1995).
35. L. B. Nelson and H. V. Poor, "Performance of multiuser detection for optical CDMA—Part II: asymptotic analysis," IEEE Trans. Commun. **43**, 3015–3024 (1995).
36. S. Zahedi and J. A. Salehi, "Analytical comparison of various fiber-optic CDMA receiver structures," J. Lightwave Technol. **18**, 1718–1727 (2000).
37. H. M. H. Shalaby, "Complexity, error probabilities, and capacities of optical OOK-CDMA communication systems," IEEE Trans. Commun. **50**, 2009–2015 (2002).
38. J. J. Chen and G. Yang, "CDMA fiber-optic systems with optical hard limiters," J. Lightwave Technol. **19**, 950–958 (2001).
39. R. Forouzan, J. A. Salehi, and M. Nasiri-Kenari, "Frame time-hopping fiber-optic code division multiple-access using generalized optical orthogonal codes," IEEE Trans. Commun. **50**, 1971–1983 (2002).
40. R. A. Scholtz, "Multiple access with time-hopping impulse modulation," in *Proceedings of the IEEE Military Communications Conference (MILCOM'93)* (IEEE, 1993), pp. 447–450.
41. W. Lam and A. M. Hussain, "Performance analysis of direct detection optical CDMA communication systems with avalanche photodiodes," IEEE Trans. Commun. **40**, 810–820 (1992).
42. T. K. Tang and K. Ben Letaief, "Bit-error rate computation of optical CDMA communication systems by large deviation theory," IEEE Trans. Commun. **46**, 1422–1428 (1998).
43. H. M. Kwon, "Optical orthogonal code-division multiple-access system—Part II: multibits/sequence-period OCDMA," IEEE Trans. Commun. **42**, 2470–2479 (1994).
44. M. Razavi and J. A. Salehi, "Statistical analysis of fiber-optic CDMA communication systems—Part I: device modeling," J. Lightwave Technol. **20**, 1304–1316 (2002).
45. J. G. Zhang, L. K. Chen, W. C. Kwong, K. W. Cheung, and A. B. Sharma, "Experiments on high-speed all-optical code-division multiplexing systems using all-serial encoders and decoders for 2 prime code," IEEE J. Sel. Top. Quantum Electron. **5**, 368–375 (1999).
46. R. F. Ormondroyd and M. M. Mustapha, "Optically orthogonal CDMA system performance with optical amplifier and photodetector noise," IEEE Photon. Technol. Lett. **11**, 617–619 (1999).
47. V. K. Jain and G. De Marchis, "Performance evaluation of optical code division multiple access networks," J. Opt. Commun. **21**, 110–115 (2000).
48. M. Razavi and J. A. Salehi, "Statistical analysis of fiber-optic CDMA communication systems—Part II: incorporating multiple optical amplifiers," J. Lightwave Technol. **20**, 1317–1328 (2002).
49. E. Desurvire, *Erbium-Doped Fiber Amplifiers, Principles and Applications* (Wiley, 1994).
50. A. Polydoros, "On the synchronization aspect of direct-sequence spread spectrum systems," Ph.D. dissertation (University of Southern California, 1982).
51. A. Polydoros and C. L. Weber, "A unified approach to serial-search spread spectrum code acquisition—Part I: general theory," IEEE Trans. Commun. **COM-32**, 542–549 (1984).
52. M. K. Simon, J. K. Omura, R. A. Scholtz, and B. K. Levitt, *Spread Spectrum Communications* (Computer Science Press, 1985), Vol. 3.

53. G. C. Yang, "Performance analysis for synchronization and system on CDMA optical fiber networks," IEICE Trans. Commun. **E77B**, 1238–1248 (1994).
54. M. M. Mustapha and R. F. Ormondroyd, "Performance of a serial-search synchronizer for fiber-based optical CDMA systems in the presence of multi-user interference," Proc. SPIE **3899**, 297–306 (1999).
55. M. M. Mustapha and R. F. Ormondroyd, "Dual-threshold sequential detection code synchronization for an optical CDMA network in presence of multi-user interference," J. Lightwave Technol. **18**, 1742–1748 (2000).
56. M. M. Mustapha and R. F. Ormondroyd, "Effect of multiaccess interference on code synchronization using a sequential detector in an optical CDMA LAN," IEEE Photon. Technol. Lett. **12**, 1103–1105 (2000).
57. A. Keshavarizan and J. A. Salehi, "Optical orthogonal code acquisition in fiber-optic CDMA systems via the simple serial-search method," IEEE Trans. Commun. **50**, 473–483 (2002).
58. A. Keshavarizan and J. A. Salehi, "Multiple-shift code acquisition of optical orthogonal codes in optical CDMA systems," IEEE Trans. Commun. **53**, 687–697 (2005).
59. B. M. Ghaffari, M. D. Matinfar, and J. A. Salehi, "Wireless optical CDMA LAN, Part I: digital design concepts," IEEE Trans. Commun. (to be published).
60. M. Dale and R. M. Gagliardi, "Analysis of fiber-optic code-division multiple access," CSI Tech. Rep. 92-06-10 (University Southern California, 1992).
61. H. M. H. Shalaby, "Performance analysis of optical synchronous CDMA communication systems with PPM signaling," IEEE Trans. Commun. **43**, 624–634 (1995).
62. H. M. H. Shalaby, "Performance analysis of optical overlapping PPM-CDMA communication systems," J. Lightwave Technol. **17**, 426–433 (1999).
63. H. M. H. Shalaby, "Direct detection optical overlapping PPM-CDMA communication systems with double optical hardlimiters," J. Lightwave Technol. **17**, 1158–1165 (1999).
64. C.-S. Bres, I. Glesk, R. J. Runser, T. Banwell, P. R. Prucnal, and W. C. Kwong, "Novel *M*-ary architecture for optical CDMA using pulse position modulation," in *Proceedings of the 18th Annual Meeting of the IEEE Lasers and Electro-Optics Society (LEOS 2005)* (IEEE, 2005) pp. 982–983.
65. A. J. Mendez, V. J. Hernandez, R. M. Gagliardi, C. V. Bennett, and W. J. Lennon, "Development of pulse position modulation/optical CDMA (PPM/O-CDMA) for Gb/s fiber optic networking," in *Proceedings of the IEEE Conference Avionics Fiber-Optics and Photonics* (IEEE, 2006), pp. 28–29.
66. G. Vannucci, "Combining frequency-division and code-division multiplexing in a high-capacity optical network," IEEE Netw. Mag. **3**, 21–30 (1989).
67. L. Tancevski and I. Andonovic, "Wavelength hopping/time spreading code division multiple access systems," Electron. Lett. **30**, 1388–1390 (1994).
68. G. C. Yang and W. C. Kwong, "Performance comparison of multiwavelength CDMA and WDMA+CDMA for fiber-optic networks," IEEE Trans. Commun. **45**, 1426–1434 (1997).
69. E. S. Shivaleela, K. N. Sivarajan, and A. Selvarajan, "Design of a new family of two-dimensional codes for fiber-optic CDMA networks," J. Lightwave Technol. **16**, 501–508 (1998).
70. E. S. Shivaleela, A. Selvarajan, and T. Srinvas, "Two-dimensional optical orthogonal codes for fiber-optic CDMA networks," J. Lightwave Technol. **23**, 647–654 (2005).
71. R. M. H. Yim, L. R. Chen, and J. Bajcsy, "Design and performance of 2-D codes for wavelength-time optical CDMA," IEEE Photon. Technol. Lett. **14**, 714–716 (2002).
72. R. M. H. Yim, J. Bajcsy, and L. R. Chen, "A new family of 2-D wavelength-time codes for optical CDMA with differential detection," IEEE Photon. Technol. Lett. **15**, 165–167 (2003).
73. H. Fathallah, L. A. Rusch, and S. LaRochelle, "Passive optical fast frequency-hop CDMA communications system," J. Lightwave Technol. **17**, 397–405 (1999).
74. J. Mendez, R. M. Gagliardi, V. J. Hernandez, C. V. Bennett, and W. J. Lennon, "Design and performance analysis of wavelength/time (W/T) matrix codes for optical CDMA," J. Lightwave Technol. **21**, 2524–2533 (2003).
75. W. C. Kwong and G.-C. Yang, "Extended carrier-hopping prime codes for wavelength-time optical code-division multiple access," IEEE Trans. Commun. **52**, 1084–1091 (2004).
76. T.-W. F. Chang and E. H. Sargent, "Optimizing spectral efficiency in multi-wavelength optical CDMA system," IEEE Trans. Commun. **51**, 1442–1445 (2003).
77. J. Mendez, R. M. Gagliardi, V. J. Hernandez, C. V. Bennett, and W. J. Lennon, "High-performance optical CDMA system based on 2-D optical orthogonal codes," J. Lightwave Technol. **22**, 2409–2419 (2004).
78. P. Saghari, R. Omrani, A. E. Willner, and P. V. Kumar, "Analytical interference model for two-dimensional (time–wavelength) asynchronous O-CDMA systems using various receiver structures," J. Lightwave Technol. **23**, 3260–3269 (2005).
79. J. Mendez, C. A. Finnila, and R. M. Gagliardi, "Wavelength division multiplexing/code division multiple access hybrid," U.S. patent 6,025,944 (February 15, 2000).
80. R. N. Nogeira, P. S. Taluja, A. L. X. Teixera, P. S. B. Andre, J. F. Rocha, and J. L. Pinto, "New technique for implementing multiwavelength orthogonal codes for OCDMA using fiber Bragg gratings written in high birefringence fibers," in *Proceedings of the 16th Annual Meeting of the IEEE Lasers and Electro-Optics Society (LEOS'03)* (IEEE, 2003), Vol. 2, pp. 545–546.
81. J. E. McGeehan, S. M. R. M. Nezam, P. Saghari, A. E. Willner, R. Omrani, and P. V. Kumar, "Experimental demonstration of OCDMA transmission using a three-dimensional (time-wavelength-polarization) codeset," J. Lightwave Technol. **23**, 3282–3289 (2005).
82. X. Wang and K. Kitayama, "Analysis of beat noise in coherent and incoherent time-spreading OCDMA," J. Lightwave Technol. **22**, 2226–2235 (2004).

83. T. Pu, H. Zhang, Y. Guo, M. Xu, and Y. Li, "Evaluation of beat noise in OCDMA system with non-Gaussian approximated method," J. Lightwave Technol. **24**, 3574–3582 (2006).
84. C.-S. Bres, Y.-K. Huang, D. Rand, I. Glesk, P. R. Prucnal, T. Bazan, C. Michie, D. Harle, and I. Andonovic, "On the experimental characterization of beat noise in 2-D time-spreading wavelength-hopping OCDMA systems," IEEE Photon. Technol. Lett. **18**, 2314–2316 (2006).
85. M. Shirasaki, "Large angular dispersion by a virtually imaged phased array and its application to a wavelength demultiplexer," Opt. Lett. **21** 366–368 (1996).
86. S. Etemad, P. Toliver, R. Menendez, J. Young, T. Banwell, S. Galli, J. Jackel, P. Delfyett, C. Price, and T. Turpin "Spectrally efficient optical CDMA using coherent phase-frequency coding," IEEE Photon. Technol. Lett. **17**, (2005).
87. A. Grunet-Jepsen, A. E. Johnson, E. S. Maniloff, T. W. Mossberg, M. J. Munroe, and J. N. Sweetser, "Demonstration of all-fiber sparse lightwave CDMA based on temporal phase encoding," IEEE Photon. Technol. Lett. **11**, 1283–1285 (1999).
88. H. Tsuda, H. Takenouchi, T. Ishii, K. Okamoto, T. Goh, K. Sato, A. Hirano, T. Kurokawa, and C. Amano, "Spectral encoding and decoding of 10 Gbit/s femtosecond pulses using high resolution arrayed-waveguide grating," Electron. Lett. **35**, 1186–1187 (1999).
89. J. Chen, R. G. Broeke, Y. Du, J. Cao, N. Chubun, P. Bjeletich, F. Olsson, S. Lourdudoss, R. Welty, C. Reinhardt, P. L. Stephan, and S. J. B. Yoo, "Monolithically integrated InP-based photonic chip development for O-CDMA systems," IEEE J. Sel. Top. Quantum Electron. **11**, 66–77 (2005).
90. C. Jing, R. G. Broeke, N. K. Fontaine, C. Ji, Y. Du, N. Chubun, K. Aihara, A.-V. Pham, F. Olsson, S. Lourdudoss, and S. J. Ben Yoo, "Demonstration of spectral phase O-CDMA encoding and decoding in monolithically integrated arrayed-waveguide-grating-based encoder," IEEE Photon. Technol. Lett. **18**, 2602–2604 (2006).
91. A. Agarwal, P. Toliver, R. Menendez, T. Banwell, J. Jackel, and S. Etemad, "Spectrally efficient six-user coherent OCDMA system using reconfigurable integrated ring resonator circuits," IEEE Photon. Technol. Lett. **18**, 1952–1954 (2006).
92. N. Wada and K. Kitayama, "A 10 Gb/s optical code division multiplexing using 8-chip optical bipolar code and coherent detection," J. Lightwave Technol. **17**, 1758–1765 (1999).
93. P. C. Teh, P. Petropoulos, M. Ibsen, and D. J. Richardson, "A comparative study of the performance of seven and 63-chip optical code-division multiple-access encoders and decoders based on superstructured fiber Bragg gratings," J. Lightwave Technol. **19**, 1352–1365 (2001).
94. T. Hamanaka, X. Wang, N. Wada, A. Nishiki, and K. Kitayama, "Ten-user truly asynchronous gigabit OCDMA transmission experiment with a 511-chip SSFBG en/decoder," J. Lightwave Technol. **24**, 95–102 (2006).
95. N. Wada, H. Sotobayashi, and K. Kitayama, "Error-free 100 km transmission of 10 Gb/s optical code division multiplexing using BPSK picoseconds-pulse code sequence with novel time-gating detection," IEE Electron. Lett. **35**, 833–834 (1999).
96. R. P. Scott, W. Cong, V. J. Hernandez, K. Lei, B. H. Kolner, J. P. Heritage, and S. J. Ben Yoo, "An eight user time-slotted SPECTS O-CDMA testbed: demonstration and simulations," J. Lightwave Technol. **23**, 3232–3240 (2005).
97. Z. Jiang, D. S. Seo, S.-D. Yang, D. E. Leaird, R. V. Roussev, C. Langrock, M. M. Fejer, and A. M. Weiner, "Four-user, 2.5-Gb/s, spectrally coded OCDMA system demonstration using low-power nonlinear processing," J. Lightwave Technol. **23**, 143–158 (2005).
98. G. P. Agrawal, *Nonlinear Fiber Optics* (Academic, 2001).
99. H. P. Sardesai, C.-C. Chang, and A. M. Weiner, "A femtosecond code-division multiple-access communication system," J. Lightwave Technol. **16**, 1953–1964 (1998).
100. R. P. Scott, W. Cong, K. Li, V. J. Hernandez, B. H. Kolner, J. P. Heritage, and S. J. Ben Yoo, "Demonstration of an error-free 4×10 Gb/s multiuser SPECTS O-CDMA network testbed," IEEE Photon. Technol. Lett. **16**, 2186–2188 (2004).
101. J. H. Lee, P. C. Teh, Z. Yusoff, M. Ibsen, W. Belardi, T. M. Monro, and D. J. Richardson, "A holey fiber-based nonlinear thresholding device for optical CDMA receiver performance enhancement," IEEE Photon. Technol. Lett. **14**, 876–878 (2002).
102. X. Wang, T. Hamanaka, N. Wada, and K. Kitayama, "Dispersion-flattened-fiber based optical thresholder for multiple-access-interference suppression in OCDMA system," Opt. Express **13**, 5499–5505 (2005).
103. J. H. Lee, P. C. Teh, P. Petropoulos, M. Ibsen, and D. J. Richardson, "A grating-based OCDMA coding-decoding system incorporating a nonlinear optical loop mirror for improved code recognition and noise reduction," J. Lightwave Technol. **20**, 36–46 (2002).
104. B. Ni and J. S. Lehnert, "Performance of a nonlinear receiver for the ultrashort-pulse optical CDMA system," Proc. SPIE **5908**, 243–252 (2005).
105. Y. Igarashi and H. Yashima, "Performance analysis of coherent ultrashort light pulse CDMA communication systems with nonlinear optical thresholder," IEICE Trans. Commun. **E89-B**, 1205–1213 (2006).
106. H. Folliot, M. Lynch, A. L. Bradley, T. Krug, L. A. Dunbar, J. Hegarty, J. F. Dunegan, and L. P. Barry, "Two-photon-induced photoconductivity enhancement in semiconductor microcavities: a theoretical investigation," J. Opt. Soc. Am. B **19**, 2396–2402 (2002).
107. F. R. Laughton, J. H. Marsh, D. A. Barrow, and E. L. Portnoi, "The two-photon absorption semiconductor waveguide autocorrelator," IEEE J. Quantum Electron. **30**, 838–845 (1994).
108. Z. Zheng, A. M. Weiner, J. H. Marsh, and M. M. Karkhanehchi, "Ultrafast optical thresholding based on two-photon absorption GaAs waveguide photodetectors," IEEE Photon. Technol. Lett. **9**, 493–495 (1997).
109. Z. Zheng, S. Shen, H. Sardesai, C.-C. Chang, J. H. Marsh, M. M. Karkhanehchi, and A. M.

Weiner, "Ultrafast two-photon absorption optical thresholding of spectrally coded pulses," Opt. Commun. **167**, 225–233 (1999).
110. K. Jamshidi and J. A. Salehi, "Statistical characterization and bit-error rate analysis of lightwave systems with optical amplification using two-photon-absorption receiver structures," J. Lightwave Technol. **24**, 1302–1316 (2006).
111. K. Jamshidi and J. A. Salehi, "Performance analysis of spectral-phase-encoded optical CDMA system using two-photon-absorption receiver structure for asynchronous and slot-level synchronous transmitters," J. Lightwave Technol. **25**, 1638–1645 (2007).
112. W. H. Glenn, "Second-harmonic generation by picosecond optical pulses," IEEE J. Quantum Electron. **QE-5**, 284–290 (1969).
113. Z. Zheng and A. M. Weiner, "Coherent control of second harmonic generation using spectrally phase coded femtosecond waveforms," Chem. Phys. **267**, 161–171 (2001).
114. Z. Zheng, A. M. Weiner, K. R. Parameswaran, M. H. Chou, and M. M. Fejer, "Low power spectral phase correlator using periodically poled $LiNbO_3$ waveguides," IEEE Photon. Technol. Lett. **13**, 82–84 (2001).
115. H. Sotobayashi and K. Kitayama, "Optical code based label swapping for photonic routing," IEICE Trans. Commun. **E83-B**, 2341–2347 (2000).
116. K. Kitayama and M. Murata, "Photonic access node using optical code-based label processing and its applications to optical data networking," J. Lightwave Technol. **19**, 1401–1415 (2001).
117. N. Wada and K. Kitayama, "Photonic IP routing using optical codes: 10 Gbits/s optical packet transfer experiment," in *Proceedings of the Optical Fiber Communication Conference (OFC'99)* (IEEE, 1999), paper WM51.
118. K. Kitayama and M. Murata, "Versatile optical code-based MPLS for circuit, burst, and packet switching," J. Lightwave Technol. **21**, 2753–2764 (2003).
119. Z. Jiang, D. S. Seo, D. E. Leaird, R. V. Roussev, C. Langrock, M. M. Fejer, and A. M. Weiner, "Reconfigurable all-optical code translation in spectrally phase-coded O-CDMA," J. Lightwave Technol. **23**, 1979–1990 (2005).
120. G. Cincotti, "Full optical coders/decoders for photonic IP routers," J. Lightwave Technol. **22**, 337–342 (2004).
121. G. Cincotti, "Design of optical full encoders/decoders for code-based photonic routers," J. Lightwave Technol. **22**, 1642–1650 (2004).
122. F. Farnoud, M. Ibrahimi, and J. A. Salehi, "A packet-based photonic label switching router for a multi-rate all-optical CDMA based GMPLS switch," IEEE J. Sel. Top. Quantum Electron. **13** (to be published).
123. C. S. Hsu and V. O. K. Li, "Performance analysis of slotted fiber-optic code-division multiple-access (CDMA) packet networks," IEEE Trans. Commun. **45**, 819–828 (1997).
124. C. S. Hsu and V. O. K. Li, "Performance analysis of unslotted fiber-optic code-division multiple-access (CDMA) packet networks," IEEE Trans. Commun. **45**, 978–987 (1997).
125. A. Stock and E. H. Sargent, "System performance comparison of optical CDMA and WDMA in a broadcast local area network," IEEE Commun. Lett. **6**, 409–411 (2002).
126. M. R. Dale and R. M. Gagliardi, "Channel coding for asynchronous fiberoptic CDMA communications," IEEE Trans. Commun. **43**, 2485–2492 (1995).
127. J. Y. Kim and H. V. Poor, "Turbo-coded packet transmission for an optical CDMA network," J. Lightwave Technol. **LT-18**, 1905–1916 (2000).
128. H. M. H. Shalaby, "Optical CDMA random access protocols with and without pretransmission coordination," J. Lightwave Technol. **21**, 2455–2462 (2003).
129. H. M. H. Shalaby, "Performance analysis of an optical CDNA random access protocol," J. Lightwave Technol. **22**, 1233–1241 (2004).
130. M. A. A. Mohamed, H. M. H. Shalaby, and E. A. Badawy, "Optical CDMA protocol with selective retransmission," in *Proceedings of the 9th IEEE Symposium on Computers and Communications (ISCC, 2004)* (IEEE, 2004), Vol. 2, pp. 621–626.
131. M. A. A. Mohamed, H. M. H. Shalaby, and E. A. Badawy, "Performance analysis of an optical CDMA MAC protocol with variable-size sliding window," J. Lightwave Technol. **24**, 3590–2462 (2003).
132. T. Koonen, "Fiber to the home/fiber to the premises: what, where, and when?," Proc. IEEE **94**, 911–934 (2006).
133. T. Pfeiffer, B. Deppisch, M. Witte, R. Heidemann, and J. P. Elbers, "An optical access system with 8 asynchronous transmitters and >1 Gbit/s network capacity," in *Proceedings of the 24th European Conference on Optical Communication* (IEEE, 1998), Vol. 1, pp. 539–540.
134. J. P. Elbers, C. Glingener, J. Kissing, E. Voges, and T. Pfeiffer, "Performance evaluation of a CDMA system using broadband sources," in *Proceedings of the 24th European Conference on Optical Communication* (IEEE, 1998), Vol. 1, pp. 341–342.
135. T. Pfeiffer, J. Kissing, J. P. Elbers, B. Deppisch, M. Witte, H. Schmuck, and E. Voges, "Coarse WDM/CDM/TDM concept for optical packet transmission in metropolitan and access networks supporting 400 channels at 2.5 Gb/s peak rate," J. Lightwave Technol. **18**, 1928–1938 (2000).
136. H. Schmuck, M. Witte, B. Deppisch, T. Pfeiffer, H. Haisch, P. Schreiber, B. Hofer, and J. Kissing, "Bidirectional optical code division multiplexed field trial system for the metro and access area," in *Proceedings of the Optical Fiber Communication Conference and Exhibit (OFC 2001)* (IEEE, 2001), Vol. 3, pp. WG4-1–WG4-3 (2001).
137. K. Kitayama, X. Wang, and H. Sotobayashi, "Gigabit-Symmetric FTTH-OCDMA over WDM PON," in *Proceedings of the Conference on Optical Network Design and Modeling* (IEEE, 2005), pp. 273–281.

138. K. Kitayama, X. Wang, and N. Wada, "OCDMA over WDM PON—Solution path gigabit-symmetric FTTH," J. Lightwave Technol. **24**, 1654–1662 (2006).
139. F. R. Gfeller and U. H. Bapst, "Wireless in-house data communication via diffuse infrared radiation," Proc. IEEE **67**, 1474–1486 (1979).
140. J. M. Kahn and J. R. Barry, "Wireless infrared communications," Proc. IEEE **85**, 265–298 (1997).
141. M. R. Pakravan and M. Kavehrad, "Design considerations for broadband indoor infrared wireless communication systems," Int. J. Wireless Information Networks **2**, 223–238 (1995).
142. J. M. H. Elmirghani and R. A. Cryan, "Indoor infrared LAN's with multiple access facilities based on hybrid PPM CDMA," in *Proceedings of the IEEE (ICC'95) International Conference on Communications* (IEEE, 1995), Vol. 2, pp. 731–734.
143. G. W. Marsh and J. M. Kahn, "Channel reuse strategies for indoor infrared wireless communications," IEEE Trans. Commun. **45**, 1280–1290 (1997).
144. S. Zahedi, J. A. Salehi, and M. Nasiri-Kenari, "A photon counting approach to the performance analysis of indoors wireless infrared CDMA networks," in *Proceedings of the 11th IEEE International Symposium on Personal, Indoor and Mobile Radio Communications (PIMRC'00)* (IEEE, 2000), Vol. 2, pp. 928–932.
145. S. Zahedi, J. A. Salehi, and M. Nasiri-Kenari, "*M*-ary infrared CDMA for indoors wireless communications," in *Proceedings of IEEE International Symposium on Personal, Indoor and Mobile Radio Communications (PIMRC'01)* (IEEE, 2001), Vol. 2, pp. 6–10.
146. B. M. Ghaffari, M. D. Matinfar, and J. A. Salehi, "Wireless optical CDMA LAN part I: digital design concepts," IEEE Trans. Commun. (to be published).
147. A. Aminzadeh-Gohari and M. R. Pakravan, "Analysis of power control for indoor wireless infrared CDMA communication," in *Proceedings of the 25th IEEE Performance, Computing, and Communications Conference (IPCCC)* (IEEE, 2006), pp. 297–302.
148. A. Aminzadeh-Gohari and M. R. Pakravan, "Power control to enable QoS for indoor wireless infrared CDMA networks," in *Proceedings of the First International Conference on Communications and Electronics (ICCE'06)* (IEEE, 2006), Vol. 1, pp. 246–252.
149. P. Azmi, M. Nasiri-Kenari, and J. A. Salehi, "Low-rate super-orthogonal channel coding for fiber-optic CDMA communication systems," J. Lightwave Technol. **19**, 847–857 (2001).
150. T. Ohtsuki, "Performance analysis of atmospheric optical PPM CDMA systems," J. Lightwave Technol. **21**, 406–411 (2003).
151. B. Hamzeh and M. Kavehrad, "OCDMA-coded free-space optical links for wireless optical-mesh networks," IEEE Trans. Commun. **52**, 2165–2174 (2004).
152. M. Jazayerifar and J. A. Salehi, "Atmospheric optical CDMA communication systems via optical orthogonal codes," IEEE Trans. Commun. **54**, 1614–1623 (2006).